Methodological Advances in the Examination of the Dopamine System in Brain

by

Judit Sóvágó

Karolinska Institutet

Stockholm 2005

From the Department of Clinical Neuroscience, Psychiatry Section
Karolinska Institutet, Stockholm, Sweden

Methodological Advances in the Examination of the Dopamine System in Brain

by

Judit Sóvágó

Karolinska Institutet

Stockholm 2005

ISBN 91-7140-552-6

Published by Karolinska University Press
Printed by Universitetsservice US-AB
Box 200, SE-171 77 Stockholm, Sweden

ABSTRACT

The dopamine (DA) system in brain has attracted considerable attention in neuroscience due to its involvement in fundamental brain functions and its postulated role in the pathophysiology of several neuropsychiatric disorders. Radioligand binding techniques *in vitro* and *in vivo*, such as receptor binding autoradiography and positron emission tomography (PET) have substantially contributed to our understanding of the DA system. With the aid of these methodologies the distribution, density and affinity of dopamine receptors can be examined in the brain at physiological conditions and in neuropsychiatric disorders. More recent aspects of research on DA receptors are the examination of coupling between DA receptors and G proteins, selective labelling of different DA receptor subtypes and *in vivo* examination of DA receptors in small regions of the human brain with minute receptor densities. Examination of the aforementioned aspects of the DA system necessitates the establishment of new techniques to study DA receptors. The aim of the present thesis was to apply and evaluate new *in vitro* and *in vivo* imaging methods for the examination of dopamine-D_2/D_3 receptors in the brain with special attention to the following three topics: (i) examination of the interaction between D_2/D_3 receptors and G proteins in human brain *in vitro*, (ii) selective visualization of D_3 receptors with PET, and (iii) improvement of the accuracy in PET imaging of D_2/D_3 receptors by correction for partial volume effects (PVEs).

In the first study agonist stimulated [^{35}S]GTPγS binding autoradiography was established for the examination of D_2/D_3 receptors in the *postmortem* human brain. The functional response to DA, the physiological agonist, and quinpirole, a prototype D_2/D_3 agonist was described in human whole hemisphere cryosections. The stimulatory effect of DA was primarily mediated by D_2/D_3 receptors. Both DA and quinpirole stimulated [^{35}S]GTPγS binding to the highest level in the striatum. Moderate to low stimulation was observed in other brain regions, such as substantia nigra, thalamus, amygdala, hippocampus and anterior cingulate. The results indicate that this method could be a suitable tool for examination of coupling between D_2/D_3 receptors and G proteins in neuropsychiatric diseases.

The aim of the next two studies was to develop a radioligand for selective *in vivo* labelling of D_3 receptors by PET. As currently no D_3-selective radioligands are available for *in vivo* examinations, the binding of the putative D_3-selective radioligand, [^{11}C]RGH-1756, was evaluated in the monkey brain. Despite the promising *in vitro* characteristics of the molecule, [^{11}C]RGH-1756 yielded very low signal for specific D_3 binding in the monkey brain. Pretreatment experiments with unlabelled RGH-1756 and raclopride showed some, albeit low, saturable binding of the radioligand. It has previously been suggested that endogenous DA occupies D_3 receptors to a high degree, which could prevent binding of [^{11}C]RGH-1756. To test this hypothesis the effect of reserpine induced DA depletion was examined on the binding of [^{11}C]RGH-1756 in the monkey brain. Following reserpine treatment there was no consistent increase in specific binding of [^{11}C]RGH-1756. This observation does not support the assumption that binding of [^{11}C]RGH-1756 to D_3 receptors is inhibited by high occupancy of D_3 receptors by endogenous DA. The most likely reason for low specific binding of [^{11}C]RGH-1756 is therefore the insufficient *in vivo* affinity of the radioligand.

In the final two studies the influence of PVE was estimated in PET studies using the D_2/D_3 selective radioligands, [^{11}C]FLB 457 and [^{11}C]raclopride in human subjects. Kinetic rate constants, binding potential (BP) and total volume of distribution (DV_{tot}) were derived from the standard two-tissue compartment model before and after PVE correction. The results demonstrated that underestimation of regional radioactivity concentration and contamination of time activity curves by spill-in of radioactivity from neighbouring regions have substantial effects on quantitative PET measurements with [^{11}C]FLB 457 and [^{11}C]raclopride. PVE correction can therefore contribute to the accuracy of quantitative PET measurements both by compensating for loss of activity (spill-out) and influence from neighbouring regions (spill-in). Based on the results initial recommendations were formulated for the application of PVE correction particularly in clinical PET studies on disorders with structural brain abnormalities.

„Mondottam ember: küzdj' és bízva bízzál!"

Madách Imre

"Så hör min maning: Kämpa och var tröst!"

Översättning: Olof Lundgren

LIST OF PUBLICATIONS

I. Sóvágó J, Makkai B, Gulyás B, Hall H. (2005) Autoradiographic mapping of dopamine-D_2/D_3 receptor stimulated [^{35}S]GTPγS binding in the human brain. *European Journal of Neuroscience* **22**: 65-71.

II. Sóvágó J, Farde L, Halldin C, Langer O, Laszlovszky I, Kiss B, Gulyás B. (2004) Positron emission tomographic evaluation of the putative dopamine-D_3 receptor ligand, [^{11}C]RGH-1756 in the monkey brain. *Neurochemistry International* **45**: 609-617.

III. Sóvágó J, Farde L, Halldin C, Schukin E, Schou M, Laszlovszky I, Kiss B, Gulyás B. (2005) Lack of effect of reserpine-induced dopamine depletion on the binding of the dopamine-D_3 selective radioligand, [^{11}C]RGH-1756. *Brain Research Bulletin* **67**: 219-224.

IV. Sóvágó J, Farde L, červenka S, Quarantelli M, Svarer C, Valastyán I, Jučaitė A, Halldin C, Gulyás B. Increasing the accuracy of in vivo quantification of extrastriatal dopamine-D_2/D_3 receptors in the human brain by partial volume effect correction. *Manuscript.*

V. Sóvágó J, Farde L, červenka S, Halldin C, Gulyás B. Increasing the accuracy of in vivo quantification of striatal dopamine-D_2/D_3 receptors in the human brain by partial volume effect correction. *Manuscript.*

TABLE OF CONTENTS

LIST OF ABBREVIATIONS

2-TCM	Two-tissue compartment model
B_{max}	Receptor density
BP	Binding potential
cAMP	Cyclic adenosine monophosphate
CSF	Cerebrospinal fluid
DA	Dopamine
D_1-D_5	Dopamine receptor subtypes 1-5
DFV	Distance from vertex
DNA	Deoxyribonucleic acid
DTT	DL-dithiothreitol
DV_{tot}	Total volume of distribution
e^-	Electron
EGTA	Ethylene glycol-bis(2-aminoethylether)-N,N,N',N'-tetraacetic acid
FWHM	Full width at half maximum
GDP	Guanosine 5'-diphosphate
GM	Grey matter
GPCR	G protein coupled receptor
GTP	Guanosine 5'-triphosphate
[^{35}S]GTPγS	[^{35}S]Guanosine 5'-γ-thiotriphosphate
ICC	Intra-class correlation coefficient
iv	Intravenous
K_1	Rate constant for ligand transfer from plasma to tissue
k_2	Rate constant for ligand transfer from tissue to plasma
k_3	Association rate constant
k_4	Dissociation rate constant
K_d	Equilibrium dissociation constant from saturation binding
K_i	Equilibrium dissociation constant from competition binding
MR	Magnetic resonance
mRNA	Messenger ribonucleic acid
p^+ or β^+	Positron
PET	Positron emission tomography
PSF	Point spread function
PVE	Partial volume effect
ROI	Region of interest
SA	Specific radioactivity
SD	Standard deviation
SEM	Standard error of mean
SN	Substantia nigra
SPM2	Statistical parametric mapping, 2
SRTM	Simplified reference tissue model
TAC	Time activity curve
VTA	Ventral tegmental area
WM	White matter

Abbreviations used in the figures are explained in the corresponding figure legends.

1. INTRODUCTION

1.1. GENERAL INTRODUCTION

Of the several billions of neurons in the human brain only a very small fraction (0.0003%-0.0004%) use dopamine (DA) as neurotransmitter (Alvaro et al. 2001; Sedvall & Farde, 1995). Despite the small number of dopaminergic neurons in the brain, huge efforts have been focused on research on the DA system during the past half of a century. Many characteristics of the DA system have already been described, but many other aspects of DA signalling must still be examined to clarify the role of this neurotransmitter system for maintenance of normal brain function.

DA was initially considered merely as an intermediate in the biosynthesis of adrenaline, until Arvid Carlsson and co-workers showed that DA itself served as a neurotransmitter (Carlsson et al. 1958). Extensive research since then has shown that DA mediates a number of different functions in the brain including locomotor control, positive reinforcement, cognitive functions, personality traits and endocrine regulation (reviewed in Missale et al. 1998; Vallone et al. 2000). Moreover, alterations of dopaminergic neurotransmission have been implicated in the pathophysiology of neuropsychiatric disorders, such as Parkinson disease, schizophrenia and drug abuse (for additional reviews see Heimer, 2003; Kaasinen & Rinne, 2002; Sedvall & Farde, 1995; Wong, 2002).

Progress in research on the DA system is dependent on the development and validation of new methodologies that enable us to examine new aspects of this neurotransmitter system. Two approaches that revolutionized neurobiological research are receptor binding and molecular biological techniques. Several milestones in research on the DA system can be attributed to the application of both of these techniques. As our knowledge about the importance of DA system grows newer and newer questions are raised regarding unexplored but potentially important features of DA signalling. Finding an answer to these questions necessitates the establishment of new approaches for the examination of the DA system.

The focus of the present thesis is on radioligand binding techniques for examination of DA receptors *in vitro* and *in vivo*. The goals were to establish new imaging methods and to improve the existing techniques for the examination of DA receptors.

1.2. THE DOPAMINE SYSTEM

1.2.1. Dopaminergic pathways in the human brain

DA is synthesized in a few circumscribed cell groups in the mesencephalon, the diencephalon and the telencephalon. The projections originating from these nuclei form four major pathways in the brain (Figure 1).

1. The nigrostriatal pathway originates from the substantia nigra (SN) and innervates the dorsal striatum (caudate and putamen). This pathway contains about 80% of all dopaminergic projections. The nigrostriatal pathway is involved in the regulation of movement, and its degeneration causes Parkinson disease.
2. The mesocortical pathway contains axons of dopaminergic cell bodies in the ventral tegmental area (VTA), which project to different neocortical areas (frontal and temporal cortex) and anterior cingulate. This pathway is probably implicated in some aspects of learning and memory.
3. The mesolimbic pathway, which also arises from the VTA, projects to several limbic areas of the brain, including nucleus accumbens, amygdala, anterior perforated substance, piriform and entorhinal cortices. The mesolimbic pathway was proposed to be

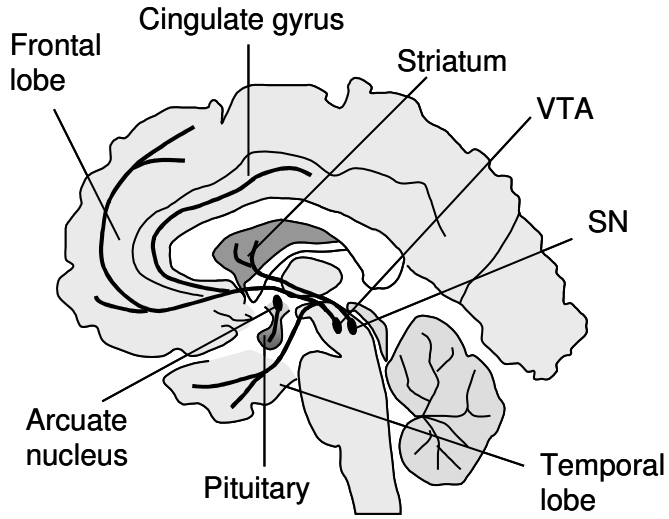

Figure 1. *The DA system in the human brain. The four major dopaminergic pathways, originating from SN, VTA and arcuate nucleus, are shown as thick, solid black lines. (Based on refs. Alvaro et al. 2001; Missale et al. 1998; Vallone et al. 2000).*

involved in motivated behaviour and emotions. However, no sharp distinction can be made between the mesocortical and the mesolimbic pathways.

4. The tuberoinfundibular pathway originates from the periventricular and arcuate nuclei in the hypothalamus and terminates in the mediane eminence of the hypothalamus. DA released from axons in this pathway is transported by the hypothalamo-hypophyseal portal system to the anterior pituitary, where it inhibits prolactin release. (Based on refs. Alvaro et al. 2001; Missale et al. 1998; Vallone et al. 2000).

1.2.2. Dopamine receptors: the discovery of multiple subtypes

DA exerts its effect by binding to specific membrane bound receptors, which belong to the family of G protein coupled receptors (GPCR). Initially two distinct subtypes of DA receptors were distinguished: D_1 receptors, which increased cyclic AMP synthesis, and D_2 receptors, which were believed not to be associated with adenylyl cyclase (for an early review see Kebabian & Calne, 1979). Soon it was demonstrated that D_2 receptors were negatively coupled to adenylyl cyclase, and receptor stimulation reduced cAMP formation (Stoof & Kebabian, 1981). Based on pharmacological evidence the existence of several types of DA receptors was suggested as early as 1979 (Kebabian & Calne, 1979). This assumption was verified by molecular biological techniques about a decade later. The cDNA for the D_3 receptor subtype was cloned and expressed in different cell lines by Sokoloff and co-workers in 1990 (Sokoloff et al. 1990). Discovery of the D_3 receptor was soon followed by the identification of two other DA receptor subtypes, the D_4 and D_5 receptor (Sunahara et al. 1991; Van Tol et al. 1991).

Based on biochemical and pharmacological properties and on sequence homology the five DA receptor subtypes are classified as D_1-like (D_1 and D_5 receptors) and D_2-like (D_2, D_3 and D_4 receptors). The five DA receptor subtypes differ in their pharmacological and biochemical characteristics, as well as in their anatomical distribution in the human brain (reviewed in Hall, 1994; Missale et al. 1998). Each DA receptor subtype is assumed to be involved in the mediation of a different set of functions in brain, and to play a role in the pathophysiology of distinct neuropsychiatric disorders, which set the need for selective examination of the functional role of DA receptors.

The present thesis focuses on two of the five identified dopamine receptor subtypes: the D_2 and the D_3 receptors.

1.2.3. Brain distribution of dopamine-D_2/D_3 receptors

1.2.3.1. Methodological considerations

Several studies, using *in vitro* or *in vivo* receptor ligand binding techniques have been performed to describe the regional distribution of D_2 and that of D_3 receptors in the brain. Selective labelling of D_2 and that of D_3 receptors is, however, hampered by the lack of selective radioligands.

Most *in vitro* and *in vivo* studies, aiming at describing the distribution and density of D_2 receptors, have utilized radioligands, which had about equal affinity for D_2 and D_3 receptors (e.g. ^{3}H or ^{11}C labelled raclopride, [^{11}C]FLB 457, [^{125}I]epidepride). In addition, all radioligands used for visualization of D_3 receptors also have some affinity for D_2 receptors (e.g. [^{3}H]7-OH-DPAT, [^{3}H]PD 128907). A possible solution for selective *in vitro* labelling of D_3 receptors is co-incubation of the tissue samples with a radioligand for D_2/D_3 receptors and a non-labelled ligand, which has higher affinity for D_2 than for D_3 receptors. Thereby the cold ligand blocks radioligand binding to D_2 receptors. Reciprocal approach can also be applied for selective visualization of D_2 receptors (Table 1). The issue of D_2 and D_3 selective radioligands is further discussed in detail below (see page 14).

In vitro receptor-binding studies can be complemented with *in situ* hybridisation experiments for the detection of mRNA. A limitation of that method is that only the somata of neurons are visualized. Another limitation is that it does not show whether the transcript is translated into the encoded protein. Therefore, mRNA mapping may show a mismatch with results of radioligand binding studies to the receptor protein.

1.2.3.2. Striatum

Within the brain the highest concentration of dopamine-D_2/D_3 receptors is expressed in the striatum. The density of D_2 receptors is similar in caudate and putamen, and the receptors are distributed evenly through the dorsoventral extent of the striatum (Gurevich & Joyce, 1999; Murray et al. 1994; Piggott et al. 1999). D_2 receptor mRNA is expressed at evenly high levels throughout the entire striatum by medium spiny neurons and large, presumably cholinergic interneurons (Gurevich & Joyce, 1999).

D_3 receptors are more abundant in the nucleus accumbens and in the ventral parts of caudate and putamen than in the dorsal part of the striatum. D_3 receptors are concentrated in the acetylcholinesterase-poor striosomal compartment within the striatum (Gurevich & Joyce, 1999; Murray et al. 1994; Piggott et al. 1999). D_3 mRNA is expressed predominantly in medium spiny neurons.

1.2.3.3. Thalamus

There are over twenty major nuclei in the thalamus. The nuclei differ in their histological, functional and biochemical characteristics, including density of D_2/D_3 receptors.

D_2 receptors are expressed at the highest density in the envelope of the thalamus, i.e. in parafascicular, parataenial, paracentral, centrolateral and centromedian nuclei (Gurevich & Joyce, 1999; Hall et al. 1996a; Rieck et al. 2004). Somewhat lower densities of D_2 receptors are expressed in the principle anterior and in the mediodorsal nuclei (Hall et al. 1996a; Kessler et al. 1993; Rieck et al. 2004). The density of D_2 receptors in the pulvinar is somewhat lower than D_2 density in the mediodorsal nucleus (Hall et al. 1996a; Kessler et al. 1993). The ventral nuclei have low-to-moderate densities of D_2 receptors (Gurevich & Joyce, 1999; Rieck et al. 2004). The expression of D_2 mRNA corresponds to that of the D_2 receptor protein (Gurevich & Joyce, 1999).

D_3 receptors are also expressed in the thalamus, and their distribution pattern is different from that of the D_2 receptors. D_3 receptors are expressed in highest density in the ante-

rior nuclei. Moderate densities of D_3 receptors are found in the mediodorsal and the ventral posterior nuclei, whereas no D_3 receptor binding has been detected in the centromedian and centrolateral nuclei. Localization of D_3 mRNA expressing cells in the thalamus has matched that of the receptor sites. Double labelling for D_2 and D_3 mRNA has revealed the presence of neurons that expressed both mRNA species throughout the thalamus (Gurevich & Joyce, 1999).

	Dopamine-D_2 receptors		***Dopamine-D_3 receptors***	
Radioligand	**[^{125}I]Epidepride[A]**	**[^{125}I]Epidepride[B]**	**[^{3}H]7-OH-DPAT[C]**	**[^{125}I]Epidepride[B]**
Blocker	**-**	**7-OH-DPAT**	**-**	**domperidone**
	B_{max} (pmol/g tissue)	B_{max} (pmol/g protein)	B_{max} (pmol/g tissue)	B_{max} (pmol/g protein)
Putamen	16.6	88-101	4	36-95
Caudate	16.5	117-155	6	10-17
Nucl. accumbens	7.2	79-101	29	51-118
Amygdala	0.9	5-39	-	9-63
Hippocampus	0.4	-	1	-
Temporal cortex	0.4	-	0	-
Ant. cingulate	0.3	-	0	-
Frontal cortex	0.2	-	-	-
Substantia nigra	-	37	7	8.4
VTA	-	26	-	64
Islands of Calleja	-	17	-	74

Table 1. *Density of dopamine-D_2/D_3 receptors measured by in vitro radioligand binding studies in selected regions of the human brain. Experimental data from: A (Kessler et al. 1993); B (Murray et al. 1994); C (Lahti et al. 1995); - Not examined.*

1.2.3.4. Cortex

The density of D_2 receptors in the cerebral cortex is generally low and only about 0.2-1.5% of the D_2 receptor density in the striatum. D_2 receptors are expressed throughout the neocortex (Camus et al. 1986; Hall et al. 1996a; Kessler et al. 1993; Olsson et al. 2004), with highest density in the temporal cortex (Kessler et al. 1993; Olsson et al. 2004).

D_3 receptors have not been detected in the neocortex (Hall et al. 1996b; Lahti et al. 1995).

1.2.3.5. Cerebellum

In the cerebellum minute densities of D_2 receptors have been reported in several studies (Camps et al. 1989; De Keyser et al. 1988; Hall et al. 1988, 1994, 1996a). In accordance with the expression of D_2 receptor protein, *in situ* hybridisation has revealed very low level of D_2 mRNA expression in the cerebellum (Hurd et al. 2001).

Observations regarding the expression of D_3 receptors in the cerebellum have mostly been made in species other than human. Hall and co-workers detected no binding of [^{3}H]PD 128907 to human cerebellar cortex, whereas [^{3}H]7-OH-DPAT showed low binding (Hall et al.

1996b). Moderate density of D_3 receptors has been measured in lobules 9-10 in the cerebellum of the rat brain using *in vitro* autoradiography (Bancroft et al. 1998; Levant, 1998; Levesque et al. 1992; Stanwood et al. 2000a). In other mammalian species, the density of D_3 receptors is much lower in lobule 9-10 of the cerebellum as compared to the rat (Levant, 1998). The role of D_3 receptors in cerebellum is controversial since this region does not receive dopaminergic innervation. D_3 receptors are presumably involved in volume transmission, and may respond to DA diffusing extrasynaptically (Diaz et al. 1995).

1.2.3.6. Other brain regions

Moderate to low level D_2 receptor expression has been observed in several other brain regions, including amygdala, hippocampus, hypothalamus, VTA, SN and globus pallidus. Within the amygdala the highest density of D_2 receptors is expressed in the basolateral and basomedial nuclei (Hall et al. 1996a; Kessler et al. 1993; Murray et al. 1994). D_2 receptors are expressed in the pars compacta of the SN and absent from the pars reticulata, whereas D_2 mRNA expression has been detected in both parts (Gurevich & Joyce, 1999). D_2 receptors in VTA and SN function as autoreceptors.

D_3 receptors are expressed in highest density in the basal forebrain, i.e. in islands of Calleja, septal nucleus and nucleus basalis (Gurevich & Joyce, 1999; Murray et al. 1994). D_3 receptors are also present in the amygdala, but their distribution pattern is different from that of the D_2 receptors, as the central nucleus and the amygdalostriatal transition zone contain more D_3 receptors than do the basal nuclei.

1.2.4. Signal transduction of D_2/D_3 receptors

1.2.4.1. D_2/D_3 receptors belong to the family of G protein coupled receptors

G protein coupled receptors (GPCR) have been named on the basis of their ability to recruit and regulate the activity of heterotrimeric G proteins. However, GPCR may not solely act via G proteins. A common structural feature of all GPCRs is the presence of seven transmembrance α-helical domains connected by alternating intracellular and extracellular loops (reiewed in Baldwin, 1993; Gether, 2000). The transmembrane helices form a crevice, which is the binding site for the physiological agonist. Small-molecule transmitters, like DA bind deep within the binding crevice, which results in activation of the receptor. The activation signal is thereafter conveyed from the GPCR to the G protein. Studies with D_2/D_3 receptor chimeras have verified the central role of the second and third intracellular loops of the receptors in the coupling to G proteins (reviewed in Baldwin, 1993; Robinson & Caron, 1996).

1.2.4.2. Interaction of D_2/D_3 receptors with G proteins

1.2.4.2.1. The structure and function of G proteins

The name ‘G protein’ refers to the ability of these molecules to bind guanine nucleotides, such as guanosine-triphosphate (GTP) and guanosine-diphosphate (GDP). Their task is to couple GPCRs to intracellular effector systems.

A heterotrimeric G protein is composed of three different polypeptide chains termed α, β and γ subunits. The α subunit binds guanine nucleotides, but all subunits can participate in signal transduction (Logothetis et al. 1987). Four major classes of G proteins are distinguished upon the α subunit: $G\alpha_s$, $G\alpha_{i/o}$, $G\alpha_q$ and $G\alpha_{12}$ (reviewed in Neer, 1995; Pennington, 1995). In the inactive state GDP is bound to the α subunit. Upon activation by the receptor the conformation of the α subunit is changed, which in turn leads to the release of GDP followed by binding of GTP. Subsequently the α subunit dissociates from the βγ-dimer

and the receptor. G proteins stay activated and can influence second messenger systems until the GTP is hydrolysed by the α subunit (Gether, 2000; Hamm, 1998, Figure 2).

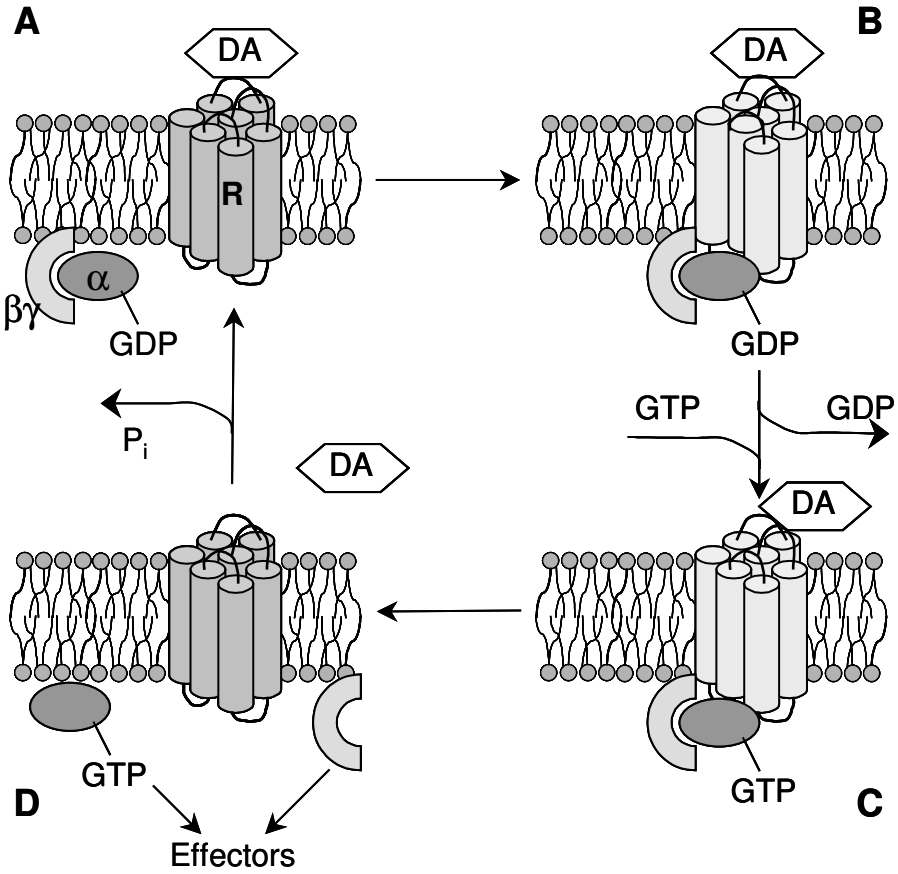

Figure 2. *Schematic drawing of GPCR activation.* **A.** *Agonist (DA) binds to the uncoupled, low-affinity state of the receptor (R), and in turn promotes and stabilises the formation of the high-affinity state, the ternary complex (***B***, with lightly shaded receptor).* **C.** *Activation of the receptor in turn results in activation of the G protein (shown here as* α *and* $\beta\gamma$ *subunits), which releases GDP and binds GTP instead***. D.** *The activated G protein dissociates from the complex and interacts with effectors. The G protein is 'turned off' by hydrolysis of GTP.*

1.2.4.2.2. Models of receptor activation

Activation of GPCRs was first explained by the ternary complex model proposed by DeLean and co-workers 25 years ago (De Lean et al. 1980). The model defines the active, high-affinity form of the receptor with a ternary complex involving the agonist, the receptor and the G protein. It also postulates that agonists are able to promote and stabilize the formation of the high-affinity state of the receptor. The reversal of the high-affinity complex to the low-affinity form involves dissociation of the G protein from the ternary complex (De Lean et al. 1980). The freed, active G protein can thereafter interact with effectors (Figure 2, 3).

The discovery of mutant GPCRs with constitutive activity lead to the extension of the model and formulation of the allosteric ternary complex model, also called two-state model (Lefkowitz et al. 1993). According to this extended model, the receptor exists in equilibrium between two states: inactive and active conformation and only the latter can interact with G

proteins. Thus, the process of receptor activation comprises at least two steps: (i) conversions from inactive to active form, and (ii) binding of G protein (Figure 3). The model proposed that ligand binding influences both steps. This model can explain the complex behaviour of various classes of ligands (agonists, partial agonists, inverse agonists, antagonists; Table 2).

It is becoming increasingly clear that the two-state model cannot sufficiently explain the complex behaviour of GPCRs. Experiments on the kinetics of receptor activation have provided strong support for the existence of multiple conformational states of GPCRs (reviewed in Gether, 2000). The 'sequential binding and conformational selection model' proposed that the receptor spontaneously alternates between different conformations (active and inactive). Binding of agonist does not occur directly to the active form but is suggested to occur sequentially, resulting in a series of conformational states that are intermediates between the active and the inactive conformations (Gether, 2000). This hypothesis, however, awaits experimental evaluation. The presented models are compared in Figure 3.

Ligand class	Mechanism of action	Intrinsic ligand efficacy	Example for D_2/D_3 receptors
Full agonist	Binds with highest affinity to R*, thereby shifts the equilibrium from R to R*. Ternary complex has maximal activity.	E ≥100%	DA NPA Quinpirole
Partial agonist	Binds with slightly higher affinity to R*, than to R, thereby shifts the equilibrium from R to R*. Ternary complex has submaximal activity.	Basal ≤ E < 100%	Apomorphine Bromocriptine Ropinirole 7-OH-DPAT PD 128907
Neutral antagonist	Binds with equal affinity to R and R*, thereby causes no change in the equilibrium.	E ≈ Basal	UH232
Inverse agonist	Stabilizes the inactive R state over R*, thereby shifts the equilibrium from R* to R.	E < Basal	Raclopride Haloperidol Clozapine Chlorpromazine Spiperol, etc.

Table 2. *Classification of DA receptor ligands according to their efficacy to activate/inhibit intracellular effector systems. Efficacy was measured either by stimulations of [^{35}S]GTPγS binding or by inhibition of forskolin stimulated cAMP accumulation. 100% efficacy is defined as the efficacy of DA. (Based on refs. Gether, 2000; Hall & Strange, 1997; Malmberg et al. 1998; Strange, 1999). Abbreviations: R, inactive receptor conformation;, R*, active conformation.*

1.2.4.2.3. Interaction of D_2/D_3 receptors with specific G proteins

In vitro studies using mutated or chimeric G proteins or knockout of individual α subunits with antibodies or antisense oligonucleotides showed that D_2 receptors are capable of coupling to multiple G proteins including $G\alpha_o$, $G\alpha_{i2}$, $G\alpha_{i3}$ (for refs. see Robinson & Caron, 1996).

The earliest observation suggested that D_3 receptors are not coupled to G proteins (Levesque et al. 1992; Sokoloff et al. 1990). Later on it was, however, verified that D_3 receptors can interact with G proteins, and that they influence second messenger systems (Chio et al. 1994; Griffon et al. 1997; Vanhauwe et al. 1999, 2000). Most observations agreed that D_3 receptors activate G proteins less effectively than D_2 receptors (Chio et al. 1994; Newman-Tancredi et al. 1999; Vanhauwe et al. 1999). D_3 receptors are capable of coupling to $G\alpha_o$ and $G\alpha_i$ proteins, but in contrast to D_2 receptors, they can also interact with $G\alpha_{q/11}$ (Newman-Tancredi et al. 1999).

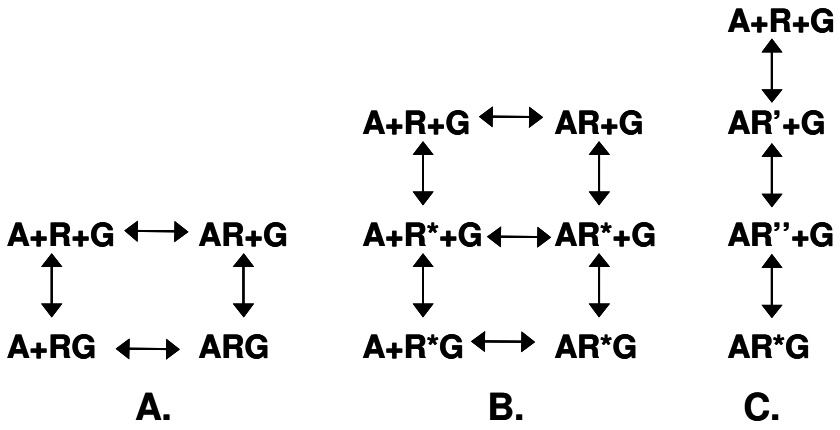

Figure 3. *Different models describing the activation process of GPCRs.* **A.** *Classic form of the ternary complex model, where the high-affinity state of the receptor corresponds to the complex of agonist (A), receptor (R) and G protein (G).* **B.** *Allosteric ternary complex model, which introduces an isomerization step (R^*, active conformation) into the process of formation of the high-affinity state.* **C.** *Sequential binding and conformational selection model, in which binding of an agonist occurs sequentially resulting in a number of conformational states of the receptor (R', R'') that are intermediates between R and R^*. The G protein may substantially affect the kinetics of the transition from AR' over AR'' to AR^*. (Based on refs. De Lean et al. 1980; Gether, 2000; Lefkowitz et al. 1993).*

1.2.4.3. Intracellular signalling pathways of D_2/D_3 receptors

The D_2 receptor was initially identified as the DA receptor subtype that is not coupled to adenylyl cyclase (Kebabian & Calne, 1979). Shortly afterwards it was shown that D_2 receptors in fact inhibit adenylyl cyclase (Stoof & Kebabian, 1981). Both D_2 and D_3 receptors can decrease intracellular cAMP level (Vanhauwe et al. 1999). In addition D_2 receptors can influence a number of other second messengers through G proteins and also via G protein independent pathways. Intracellular signalling pathways modulated by D_2 receptors are summarized in Figure 4 (reviewed in Missale et al. 1998; Robinson & Caron, 1996; Vallone et al. 2000).

Signal transductions pathways of the D_3 receptor are not described as well as those of the D_2 receptor. In some cell lines, D_3 receptor was able to inhibit Ca^{2+} currents (Seabrook et al. 1994). In CHO cells D_3 receptor was able to stimulate extracellular acidification by the Na^+/H^+ exchanger (Coldwell et al. 1999a, 1999b).

Most of the experiments that examined functional coupling of D_2/D_3 receptors were performed using cloned receptors expressed in various cell lines. The drawback of such studies is that cultured cells may not express the same G proteins or second messengers that are

found in neurons expressing D_2/D_3 receptors. It also might happen that the interaction of D_2/D_3 receptors with a certain second messenger observed in a cell line is not representative for brain D_2/D_3 receptors, as it does not normally occur in neurons. The result of experiments with cell cultures should therefore be interpreted with appropriate caution.

1.2.5. Functions of brain D_2/D_3 receptors

DA receptors mediate a number of different functions in brain, and are also involved in the pathophysiology of several neuropsychiatric disorders. The role of DA receptors under normal conditions and in neurological and psychiatric disorders has been extensively reviewed (e.g. Kaasinen & Rinne, 2002; Missale et al. 1998; Vallone et al. 2000; Wong, 2002). Without aiming for a complete overview of the overwhelmingly huge literature on the function of DA receptors in brain, only a few aspects of DA function relevant for the present work will be mentioned.

The importance of the DA system in controlling locomotion is well known. Degeneration of dopaminergic neurons in the SN causes Parkinson disease, a condition characterised by rigidity, tremor and severe disturbance of voluntary movements and that of coordination. DA is also assumed to mediate a number of higher cognitive functions and is involved in the pathophysiology of schizophrenia, a severe disabling psychiatric disorder with symptoms such as hallucinations, delusions and emotional blunting. In the following paragraphs, some DA related aspects of these two disorders will be discussed, with special emphasis on pieces of knowledge obtained from neuroimaging studies. The major results of *in vitro* and *in vivo* DA receptor binding studies are mentioned. We also point out some questions regarding the distribution and function of DA receptors in the brain, which cannot be examined with traditional neuroimaging methods but require instead the application of novel techniques.

The DA hypothesis of schizophrenia postulates that schizophrenia is related to hyperdopaminergic state in brain. Initial PET studies have shown that the density of D_2/D_3 receptors was indeed increased in the striatum of schizophrenic patients (Wong et al. 1986). Other studies, however, did not verify this observation (Farde et al. 1990). Yet other PET studies showed alterations of pre-synaptic DA function in schizophrenia (Hietala et al. 1995; Laruelle et al. 1996). *In vitro* studies, on the other hand, have demonstrated changes of intracellular signalling systems in schizophrenia, without explicitly connecting the observations to any neurotransmitter receptor (Jope et al. 1998; Okada et al. 1994; Yang et al. 1998). It is possible that the conflicting results of studies examining D_2/D_3 receptor density in the brain have been obtained because the function and not the number of receptors is changed in schizophrenia. Traditional radioligand binding techniques, however, cannot be used to examine the function of DA receptors in brain.

Experiments in animal models of Parkinson disease have demonstrated increased numbers of D_2 receptors and enhanced D_2 receptor/G protein coupling (Geurts et al. 1999; Khan et al. 1999; Newman-Tancredi et al. 2001). Some authors suggested that the augmented DA receptor/G protein coupling could contribute to the development of dopaminergic hypersensitivity, and proposed that similar regulatoy mechanisms could take place in pathophysiological conditions (Geurts et al. 1999). To challenge these hypotheses new imaging techniques are necessary, which can be used to localize receptors and measure their function at the same time.

Shortly after the discovery the D_3 receptor, the role of this receptor subtype was suggested in the pathophysiology of schizophrenia, due to the abundance of D_3 receptors in limbic brain regions. This hypothesis was confirmed by studies that examined the association between schizophrenia and polymorphism of the D_3 receptor (Schwartz et al. 2000). The the-

ory was further supported by the observation that antipsychotic drugs have about as high affinity for D_3 as for D_2 receptors (Joyce, 2001; Vanhauwe et al. 2000).

D_3 receptors are probably also involved in the pathophysiology of Parkinson disease (Joyce et al. 2002; Ryoo et al. 1998). This assumption was based on the observation that DA agonists used to treat symptoms of Parkinson disease also have high affinity for D_3 receptors (Joyce et al. 2002). According to the literature, the density of D_3 receptors was also changed in Parkinson disease (reviewed in Joyce, 2001). Examination of D_3 receptors in the human brain was, however, hampered by the lack of selective radioligands with high-affinity for the D_3 receptor.

Postmortem studies described neuronal changes in the mediodorsal nucleus of the thalamus in schizophrenic brains, and suggested that the observed alterations could play a role in the pathophysiology of the disease (Byne et al. 2002; Pakkenberg, 1990, 1992). A PET study in schizophrenic patients reported decreased D_2/D_3 receptor density in the medial thalamus (Talvik et al. 2003). In this study, the mediodorsal nucleus was not examined separately, due to the difficulties arising from the limited spatial resolution of the PET system. Examination of D_2/D_3 receptors in small regions, such as the SN, is also important in disorders such as Parkinson disease. Nevertheless, accurate measurement of D_2/D_3 receptor density in such small structures as the mediodorsal nucleus or the SN necessitates the application of special image analysis techniques, which can compensate for the inaccuracies caused by the low spatial resolution of PET.

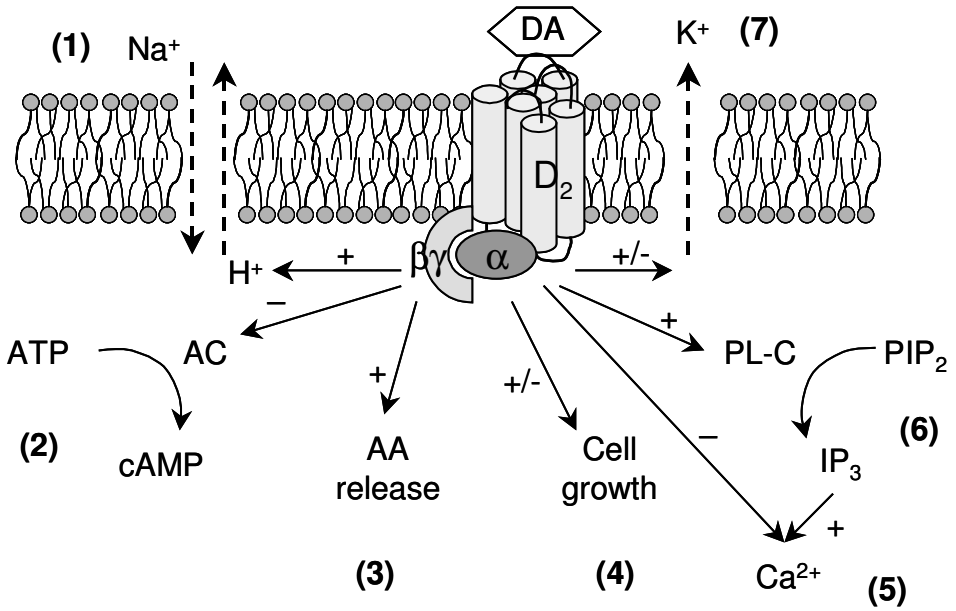

Figure 4. *Intracellular signalling pathways activated by D_2 receptors. D_2 receptors are able to (1) stimulate the Na^+/H^+ exchanger, (2) inhibit adenylyl cyclase (AC), (3) potentiate release of arachidonic acid (AA), (4) in some cell lines inhibit, in others stimulate cell growth and differentiation, (5) inhibit Ca^{2+} currents, (6) stimulate phospholipase-C, and thereby increase the production of inositol 1,4,5-trisphosphate (IP_3) from phosphatidylinositol-diphosphate (PIP_2) and subsequently elevate the level of cytoplasmatic Ca^{2+}, (7) in some cell lines inhibit, in others stimulate K^+ currents. Signs beside the arrows indicate the effect of D_2 receptor on the second messenger: +, stimulation; –, inhibition; +/–, stimulation or inhibition depending on the cell line examined.*

1.3. IMAGING TECHNIQUES FOR THE EXAMINATION OF D_2/D_3 RECEPTORS IN BRAIN

1.3.1. Why is the development of new imaging techniques necessary?

In vitro and *in vivo* neuroreceptor binding techniques, i.e. autoradiography and PET have substantially contributed to our understanding of the DA system. The history of both methodologies goes back to the mid 1970s (Seeman et al. 1975; Ter-Pogossian et al. 1975). The first experiments using autoradiography to examine DA receptors in the brain were performed by Seeman and colleagues in 1975. The first PET system that used the tomographic principle for image reconstruction was reported in the same year by Ter-Pogossian and co-workers. Both methods have been extensively used to examine the distribution and density of D_2/D_3 receptors in the human brain under normal conditions and in neuropsychiatric diseases. Traditional radioligand binding autoradiography and PET imaging techniques using D_2/D_3 selective radioligands, however, cannot answer all the questions that are still pending with regard to the distribution and function of D_2/D_3 receptors in the brain. In the present work three such questions of D_2/D_3 receptor imaging are addressed.

1. Some recent discoveries directed the attention on the first step of the intracellular signal transduction pathway activated by D_2/D_3 receptors, i.e. on the interaction of the receptors and G proteins. It has been demonstrated that D_2 and D_3 receptors activate G proteins with different efficiency in cell lines. The observation that both traditional and atypical antipsychotic drugs behave as inverse agonists at D_2/D_3 receptors further emphasized the importance of the interaction between receptors and G proteins. Traditional radioligand binding autoradiography and PET, however, provide no information about the function of the visualized receptors. A recently developed technique, agonist stimulated [^{35}S]GTPγS binding autoradiography (Sim et al. 1995), in contrast, can be used to localise GPCR in the brain and examine their interactions with G proteins.

2. The presumed different physiological role of D_2 and D_3 receptors, together with their suggested distinct role in the pathophysiology of schizophrenia and Parkinson's disease gave strong support for attempts to selectively visualize D_2 and D_3 receptors. *In vitro* studies using receptor binding autoradiography with D_3-preferring radioligands have been performed already for the examination of D_3 receptors (e.g. Bancroft et al. 1998; Hall et al. 1996b; Murray et al. 1994; Ricci et al. 1995). However, no successful *in vivo* visualization of the D_3 receptor has been carried out yet, due to the lack of selective radioligands with high-affinity for the D_3 receptor.

3. PET with D_2/D_3 selective radioligands has been used extensively to examine density of D_2/D_3 receptors in rather large regions of the human brain, such as cortical areas, striatum and thalamus. *In vitro* studies, in contrast, pointed out the importance of examination of small regions in the brain, such as thalamic nuclei or functional subdivisions of the striatum. The accuracy of PET measurements in small brain regions is compromised by the limited spatial resolution of the PET system. Special image analysis techniques are necessary for quantification of D_2/D_3 receptor binding in these regions, which can compensate for the phenomena arising from the limited spatial resolution of PET.

1.3.2. [^{35}S]GTPγS binding autoradiography

1.3.2.1. General description of the method

[^{35}S]GTPγS binding autoradiography is a novel *in vitro* imaging method to study the distribution and function of GPCRs in tissue sections. It unifies the advantages of receptor binding autoradiography and that of [^{35}S]GTPγS binding by providing information about the

distribution of receptors and the interaction of receptors and G proteins at the same time (reviewed in Sovago et al. 2001). [^{35}S]GTPγS binding has initially been used to study the activation of GPCRs in cell membranes (Lazareno, 1999). Agonist stimulated [^{35}S]GTPγS was modified so that it can also be applied to tissue sections (Sim et al. 1995).

The assay is based on guanine nucleotide exchange at G proteins upon agonist stimulation of the GPCR (Figure 2). Binding of an agonist to the receptor promotes the formation of the high-affinity, G protein coupled state of the receptor. Activation of the receptor induces activation of the G protein. The activated G protein releases GDP and binds [^{35}S]GTPγS instead. As [^{35}S]GTPγS is resistant to hydrolysis the radioligand stays bound to the G protein, and the activated receptor/G protein complex can be localized. One receptor can activate several surrounding G proteins, depending on the efficiency of the ternary complex.

The limitation of [^{35}S]GTPγS binding autoradiography is that not all GPCRs can be visualized. Presently only $G_{i/o}$ coupled receptors can be detected with this technique. Labelling of receptors with small density or low G protein coupling efficiency can also be difficult.

1.3.2.2. [^{35}S]GTPγS binding autoradiography for the examination of D_2/D_3 receptors in brain

[^{35}S]GTPγS binding autoradiography has previously been successfully applied in the examination of D_2/D_3 receptors in the rat brain (Culm et al. 2003; Febo et al. 2003; He et al. 2000; Newman-Tancredi et al. 2001). No studies, other than the one reported in the present thesis, have been performed to examine DA receptor stimulated G protein activation in human brain sections, although this assay could provide valuable information on DA receptor function under physiological conditions and in neuropsychiatric diseases.

1.3.3. Positron emission tomography

1.3.3.1. Basic principles

Positron emission tomography (PET) is a non-invasive technique to study the distribution of tracer molecules labelled with positron emitting isotopes in the body. The data obtained by detection of tracer molecules is used to reconstruct images describing the distribution of the tracer in the body (Eriksson et al. 1989).

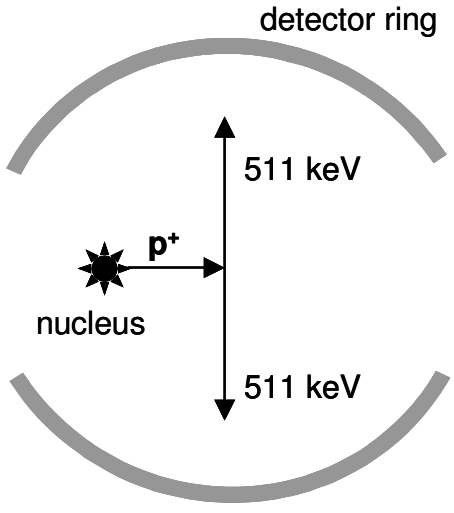

Figure 5. *Physical principles of PET. The emitted positron (p^+ or β^+) travels a short distance before annihilating with an electron (e^-). In the annihilation process two γ-photons (511 keV each) are formed, which propagate in nearly opposite directions. These two γ-photons can be detected with a pair of opposed γ-ray detectors. To ensure that the detected γ-rays originate from the same annihilation only those signals are accepted which are detected within a short (~10 nsec) timing window. This technique is called coincidence detection.*

At the time of the radioactive decay, the emitted positron (β^+ or p^+) has relatively high energy so it travels through the body, interacts with electrons (e^-) along the way, and loses energy with each interaction. When its momentum is nearly zero, it annihilates with an e^- to produce two γ-photons (511 keV), which propagate along almost collinear paths (Figure 5). The degree of non-collinearity depends on the momentum of the β^+ and e^- at the time of the annihilation. The divergence of the angle of the γ-rays from 180^o is in the order of 1^o or less, and is usually ignored. The distance the β^+ travels before annihilation is termed positron range. The magnitude of this range depends on the β^+ energy, which varies widely among isotopes, and on the tissue where the annihilation occurred (Ollinger & Fessler, 1997). The degree of non-collinearity and the positron range set the lower limit to the spatial resolution of PET systems to about 2 mm.

Two crucial characteristics of positron cameras are sensitivity and spatial resolution, which largely determine accuracy of the image data (Hoffman et al. 1986). Spatial resolution of a PET system is defined by the degree to which the representation of an object is blurred in the image (reviewed in Eberl & Zimmermann, 2004). The representation of a perfect point source in a PET image (the point spread function, PSF) can be approximated by a Gaussian function. The resolution of the system is commonly defined in terms of its full width at half maximum (FWHM), the distance where the intensity in the image drops to half of the maximal value (Figure 6). The best obtainable resolution of a PET system is called intrinsic resolution (Ollinger & Fessler, 1997). It is dependent on non-collinearity of the γ-photons, positron range and size of the detectors (Eriksson et al. 1989; Links & Wagner, 1982; Phelps et al. 1975). This resolution is rarely achieved in practice. The final resolution of the image is called reconstructed resolution (Ollinger & Fessler, 1997).

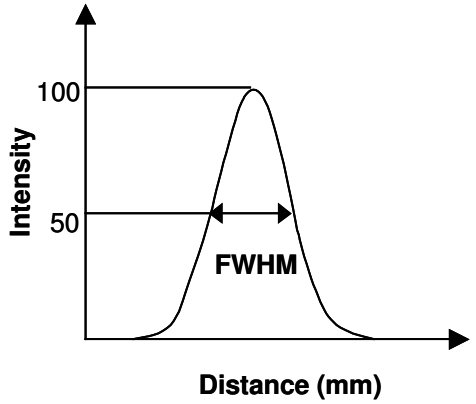

Figure 6. *Image blurring: profile of a point source.*

PET images are most commonly reconstructed using filtered backprojection, a method for tomographic image reconstruction (reviewed in Bailey & Parker, 2004; Eriksson et al. 1989; Ollinger & Fessler, 1997). In PET, the projection data measured by the detectors represent the line integrals through the radio-isotope distribution. By the mathematical process of backprojection the line-projection data are re-projected onto a 2-dimensional image matrix. If no filtering is used the reconstructed images are blurred; the phenomenon is sometimes referred to as 1/r smearing (Eriksson et al. 1989). The blurring can be removed by a filtering step before backprojection, using a ramp filter. This filter, however, accentuates noise in the data. This can be limited by the use of a noise reduction filter, such as Butterworth, Hamming or Hann filters. Thereby the reduction in noise is traded-off for some decrease in the image resolution (Bailey & Parker, 2004; Ollinger & Fessler, 1997).

1.3.3.2. Partial volume effect

The limited spatial resolution of PET systems influences quantitative PET measurements (Hoffman et al. 1979; Kessler et al. 1984; Mintun et al. 1984). The direct consequence of limited resolution is underestimation of signal from objects smaller than 2-3 times the FWHM of the PET scanner (Hoffman et al. 1979; Kessler et al. 1984). A related effect of the rather low spatial resolution of PET devices implies that activity from surrounding tissue compartments contribute to the signal measured in a volume element, i.e. activity in a region

is contaminated by activity from neighbouring regions (spill-over effect). These phenomena are commonly known as partial volume effects (PVEs; Henze et al. 1983; Herrero et al. 1989; Kessler et al. 1984; Figure 7). PVE can obscure accurate quantification of radioligand uptake in the brain, as the observed regional time-activity curves (TACs) are influenced by TACs for surrounding tissue components. Due to the complexity of models used to quantify radioligand binding, it is not possible in the individual case to predict the effect of PVE on quantitative receptor ligand binding parameters, and PVE correction has to be performed. Although several different algorithms were developed, validated and tested for PVE correction during the past fifteen years (Aston et al. 2002; Labbe et al. 1996; Meltzer et al. 1990; Muller-Gartner et al. 1992; Rousset et al. 1998a) very few studies have been performed so far to explore the effect of PVE on quantitative receptor ligand binding studies. A possible reason for the small number of such studies is that the implementation of these methods was complicated and the computational costs were high. Recently, however a number of PVE correction methods were implemented in a common software framework (Quarantelli et al. 2004), which enables relatively easy and fast application of PVE correction.

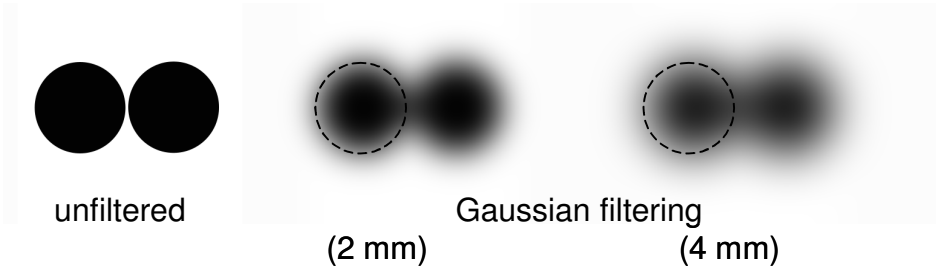

Figure 7. *Illustration of image blurring and the resulting PVEs. All circles originally have a diameter of 12 mm and homogenous intensity (blackness) within the entire circle. The circles are not overlapping. The second and third pairs of circles have been filtered with a Gaussian kernel (2 mm and 4 mm FWHM) for demonstration of blurring, virtual loss of intensity within the circles and spill-over. The dashed circles show the original size of the filled circles (12 mm diameter).*
The picture was not made from a PET image, but it illustrates the inherent blurring of PET images.

1.3.3.3. Selective visualization of D_2/D_3 receptors

PET using ^{11}C or ^{18}F labelled radioligands is a suitable tool for the examination of neurotransmitter receptors and tranporters in the brain. The development of PET radioligands is a challenging task, as the molecules have to satisfy a number of requirements regarding toxicitiy, lipophilicity, penetration of the blood-brain barrier, affinity and selectivity (reviewed in Halldin et al. 2001). At present there are several different radioligands available for D_1 and D_2-like receptors.

All currently known D_2-selective radioligands possess some affinity to D_3 receptors, and *vice versa*. Therefore, they cannot completely discriminate between D_2 and D_3 receptors. Based on their relative affinity for D_2 and D_3 receptors D_2/D_3-selective radioligands can be classified as D_2-preferring (higher affinity for D_2 than for D_3), D_3-preferring (higher affinity for D_3 than for D_2) or non-selective (about equal affinity for both subtypes; Table 3).

Selective labelling of D_3 receptors is challenged by some properties of the D_3 receptor itself. According to previous observations, D_3 receptors are expressed in a limited number of

regions in the brain, and their distribution is partially overlapping with that of the more abundant D_2 receptor, e.g. in ventral striatum, hippocampus, SN and thalamus (see details above). In these regions, signal from D_2 receptors can, therefore, obscure or confound the signal originating from D_3 receptors, unless a completely D_3-selective radioligand is used. Some authors have suggested that D_3 receptors are occupied by endogenous DA to a high degree under physiological conditions (Levant, 1995; Schotte et al. 1992, 1996). Therefore, competition with endogenous DA could prevent binding of radioligands to D_3 receptors, especially in *in vivo* studies.

Ligand	DA receptor	Tissue/ cell line	Affinity (nM)	D_2/D_3 selectivity index	References
Spiperone	D_2	CHO-hD_2	0.1[E]	0.1	(Vanhauwe et al. 1999)
	D_3	CHO-hD_3	1.0[A]		
NPA	D_2	CHO-hD_2	0.09[F]	0.4	(Seeman et al. 2005)
	D_3	CCL1-3-hD_3	0.25[F]		
IBZM	D_2	LtK$^-$-hD_2	1.6[C]	0.7	(Videbaek et al. 2000)
	D_3	HEK-293-hD_3	2.2[D]		
Raclopride	D_2	CHO-hD_2	7.5[E]	1	(Vanhauwe et al. 1999)
	D_3	CHO-hD_3	8.5[A]		
FLB 457	D_2	rat striatum	0.02[B]	1	(Halldin et al. 1995)
	D_3	CHO-hD_3	0.02[B]		
Dopamine	D_2	CHO-hD_2	22[A]	5.6	(Sokoloff et al. 1992)
	D_3	CHO-hD_3	3.9[A]		
Quinpirole	D_2	CHO-hD_2	1000[A]	10	(Coldwell et al. 1999a)
	D_3	CHO-hD_3	100[A]		
PD 128907	D_2	CHO-hD_2	20[E]	14	(Pugsley et al. 1995)
	D_3	CHO-hD_3	1.4[E]		
7-OH-DPAT	D_2	CHO-rD_2	61[A]	78	(Levesque et al. 1992)
	D_3	CHO-rD_3	0.78[A]		

Table 3. *Affinity of most commonly used ligands and that of DA for D_2 and D_3 receptors. Affinity of the ligands (K_i) was measured in competitive binding studies with the following radioligands: A, [^{125}I]iodosulpride; B, [^{125}I]NCQ 298; C, [^{3}H]spiroperidol; D, [^{3}H]7-OH-DPAT; E, [^{3}H]spiperone; F, [^{3}H]domperidone. The D_2/D_3 selectivity index was calculated as the ratio of each ligand's affinity for D_2 and for D_3 receptors. Values <1 indicate D_2 preferring ligands, whereas values >1 indicate D_3-preferring ligands. K_i values of agonists are representative for the high-affinity binding sites. hD_2/D_3, recombinant human receptors; rD_2/D_3, recombinant rat receptors.*

2. AIMS

The overall objective of the study was to apply and evaluate new *postmortem* and *in vivo* imaging methods for the examination of dopamine-D_2/D_3 receptors in the brain. The methodological developments and improvements targeted three different aspects of D_2/D_3 receptor imaging.

1. Regional examination of the interaction between D_2/D_3 receptors and G proteins. For this purpose a new method, agonist stimulated [^{35}S]GTPγS binding autoradiography was established for the examination of D_2/D_3 receptors in human brain sections (Paper I).

2. Selective visualization of D_3 receptors in the brain with PET. In this project the binding of a novel, putatively D_3 selective radioligand, [^{11}C]RGH-1756 was evaluated in the monkey brain under physiological conditions and after reserpine pretreatment (Papers II and III).

3. Improving the accuracy of *in vivo* imaging of dopamine-D_2/D_3 receptors with PET by partial volume effect correction. In this study the effect of PVE is examined on the regional parameters for [^{11}C]FLB 457 and [^{11}C]raclopride binding in the human brain. The relevance of PVE correction in pre-clinical and clinical PET studies on D_2/D_3 receptors is also discussed (Papers IV and V).

3. THEORY AND EXPERIMENTAL PROCEDURES

3.1. SUBJECTS

3.1.1. Brain tissue

Human brains were obtained *postmortem* at clinical autopsy at the National Institute of Forensic Medicine, Karolinska Institutet, Stockholm, Sweden, and at the Department of Pathology, University of Oulu, Finland (Paper I). The study was approved by the Ethics Committee at Karolinska Institutet. Tissue was obtained from six male subjects with no documented history of neurological or psychiatric disorders (age: 32-70 y, mean: 51 y, *postmortem* time: 5-48 h, mean: 21 h, storage time in brain bank: 2.5- 20 y, mean: 9 y).

3.1.2. Cynomolgus monkeys

Altogether four (1 male and 3 females) Cynomolgus monkeys participated in the examinations with [^{11}C]RGH-1756 (Papers II and III). The studies were approved by the Animal Research Ethics Committee of the Northern Stockholm Region, Sweden. The Cynomolgus monkeys (weight 3.0-8.2 kg) were supplied by the Swedish Institute for Infectious Disease Control, Solna, Sweden.

3.1.3. Human subjects

No new PET examinations involving human subjects were performed within this thesis. The PET and magnetic resonance (MR) image datasets were obtained from the comparison group in an ongoing clinical study, for which the approvals of the Research Ethics and the Radiation Safety Committees of the Karolinska Hospital have been obtained (Papers IV and V). Nine healthy volunteers (age: 57 ± 7 y, mean ± SD) were previously examined with [^{11}C]FLB 457 and [^{11}C]raclopride, and also underwent MR examination. All individuals were healthy according to medical history, physical examination, MR imaging of the brain and blood and urine chemistry.

The image datasets of all nine subjects were included in Paper IV on [^{11}C]FLB 457, whereas one subject was excluded from the analysis in Paper V on [^{11}C]raclopride, as the appropriate input function was not possible to define.

3.2. COMPOUNDS AND RADIOCHEMISTRY

[^{35}S]GTPγS (specific radioactivity, SA: 1080-1160 Ci/mmol) was purchased from Amersham Biosciences AB (Uppsala, Sweden).

Derivative RGH-1756 and its desmethyl precursor, 04512626 were synthesized at Gedeon Richter Ltd., Budapest, Hungary. [^{11}C]RGH-1756 was synthesized as previously described by O-methylation of the corresponding desmethyl precursor using [^{11}C]methyl triflate (Langer et al. 2000). SA of [^{11}C]RGH-1756 was 4-270 GBq/μmol. According to *in vitro* competitive radioligand binding studies with RGH-1756, the affinity of the compound was about 100 times higher for D_3 than for D_2 receptors (K_i against [^{3}H]spiperone was 0.12 nM at D_3 receptors, and 12.2 nM at D_{2L} and 15.2 nM at D_{2S} receptors (Kiss et al. 2000). RGH-1756 also had rather high affinity for 5-HT_{1A} receptors (K_i against [^{3}H]8-OH-DPAT was 0.96 nM).

Radiosynthesis of [^{11}C]FLB 457 and [^{11}C]raclopride was performed as described earlier (Halldin et al. 1991, 1995). SA was 39-578 GBq/μmol and 49-353 GBq/μmol for [^{11}C]FLB 457 and [^{11}C]raclopride, respectively.

All other compounds and chemicals were obtained from standard commercial sources and were of analytical grade wherever possible.

3.3. AUTORADIOGRAPHY

3.3.1. Cryosectioning

Whole hemispheres were removed, frozen and cryosectioned as described earlier (Hall et al. 1994, 1998, 2001) using a heavy-duty cryomicrotome (Leica Cryomacrocut CM3600, Leica, Nussloch, Germany). Briefly, 100 μm thick horizontal cryosections were cut parallel to the Talairach anterior commissure – posterior commissure plane (Talairach & Tournoux, 1988). The cryosections were transferred to gelatine or poly-L-lysine coated glass plates (10x22 cm), dried at room temperature and then stored with dehydrating agents at –25 ^{o}C until the experiments.

Cryosections containing the dorsal parts of caudate and putamen and thalamus (distance from vertex, DFV: 62.0-74.1 mm), ventral parts of caudate and putamen and globus pallidus (DFV: 72.1-85.6 mm), and substantia nigra (DFV: 85.5-103.1 mm), respectively, were used to study the distribution of DA receptor activated G proteins (Paper I).

3.3.2. [^{35}S]GTPγS binding autoradiography

The [^{35}S]GTPγS binding autoradiographic procedure was carried out as described previously (Sim et al. 1995) with slight modifications (Paper I). During the initial series of experiments the optimal assay conditions were defined by varying the incubation time, temperature and buffer composition. The effects of different experimental conditions on DA stimulated [^{35}S]GTPγS binding were measured in duplicates. The conditions, which resulted in the highest signal-to-noise ratio in the striatum, that is the highest stimulation over basal binding, were subsequently used to characterize agonist stimulated [^{35}S]GTPγS binding in human brain section.

The optimal assay conditions were as follows. The sections were preincubated in HEPES buffer (50 mM, pH 7.4, containing 150 mM NaCl, 75 mM KCl, 5 mM $MgCl_2$, 0.2 mM EGTA, 1 mM DTT and 2 mM GDP) for 30 min at 37 ^{o}C. The sections were subsequently incubated with 50 pM [^{35}S]GTPγS in the same buffer for 90 min at 37 ^{o}C. Basal binding was determined in the absence of agonists. DA (1 mM, in the presence of 100 μM pargyline, a selective monoamine oxidase-B inhibitor) or quinpirole (1 mM) was used to stimulate [^{35}S]GTPγS binding at DA receptors. Receptor subtype-specificity of DA stimulated [^{35}S]GTPγS binding was examined by the simultaneous addition of raclopride (100 μM) or SCH23390 (100 μM). After incubation, the sections were washed in cold HEPES buffer for 2x10 min, followed by a brief dip in ice-cold distilled water. The sections were dried on a warm plate and subsequently exposed to β-radiation sensitive film (Kodak Biomax MR, Amersham Biosciences AB, Uppsala, Sweden) for 1-2 days.

3.4. POSITRON EMISSION TOMOGRAPHY

3.4.1. PET system

Radioactivity in the brain was measured using an ECAT Exact HR PET system (CTI/Siemens, Knoxville, TN) run in three-dimensional mode. Transmission scans (10 min) were obtained with rotating ^{68}Ge/^{68}Ga sources prior to the emission scans, and were used for attenuation correction. Images were reconstructed using a Hann filter (2 mm FWHM), after

correction for attenuation, random and scattered events. The reconstructed volume was displayed as 47 image slices with an inter-slice distance of 3.125 mm.

The transaxial resolution of the system decreases from 3.6 mm FWHM at the centre of the field of view to 4.5 mm FWHM tangentially and 7.4 mm FWHM radially at 20 cm from the centre. Axial resolution is 4 mm FWHM at the center of the field of view, and 6.8 mm at 20 cm from the centre (Wienhard et al. 1994). The resolution of the PET images along the x and y axes was estimated from measurements with a ^{68}Ga/^{68}Ge rod source of 2 mm diameter. The image resolution along the z axis was calculated from the resolution of the PET system and the filter used during image reconstruction. The PSF of the PET images was estimated as 6 mm x 6 mm x 6 mm FWHM uniformly throughout the entire field of view (Papers II-V).

3.4.2. Examinations with [^{11}C]RGH-1756

The PET examinations of the Cynomolgus monkeys (Papers II and III) were essentially performed as described earlier (Karlsson et al. 1993). Anaesthesia was induced and maintained by repeated intramuscular injections of a mixture of ketamine (3-7 mg/kg/h Ketalar®, Pfizer) and xylazine hydrochloride (0.5-2 mg/kg/h Rompun®, Vet. Bayer). A venous cannula was inserted into a sural vein for administration of [^{11}C]RGH-1756. A head fixation system was used to secure a fixed position of the monkey head during the PET measurements. Heart and breath rate and rectal temperature of the monkeys were monitored continuously during the PET examinations. Body temperature was maintained by a heating blanket. The radioligand was dissolved in 4-5 ml physiological phosphate buffer (pH=7.4) and the solution was injected intravenously (iv) in 5 seconds as a single bolus. In each PET experiment 15-54 MBq of [^{11}C]RGH-1756 was administered. Radioactivity in the brain was measured according to a pre-programmed sequence of frames for up to 93 minutes after the injection of [^{11}C]RGH-1756.

In the initial experiments (Paper II) the saturability of [^{11}C]RGH-1756 binding was examined in a monkey by varying the injected mass of unlabelled RGH-1756 (0.14-0.42 μg). Specificity of [^{11}C]RGH-1756 binding was examined in pretreatment experiments by the iv administration of one of the following compounds to the monkey 15-20 min before the injection of [^{11}C]RGH-1756: unlabelled RGH-1756 (0.02 mg/kg), the dopamine-D_2 receptor antagonist raclopride (1 mg/kg), and the 5-HT_{1A} receptor antagonist WAY-100635 (0.5 mg/kg). To obtain anatomical correlates for the PET images an MRI examination of the monkey was performed using a GE Signa scanner (1.5 Tesla) with a T2 weighted sequence. Blood samples of 2.0 ml were obtained from the femoral vein of the monkey 5, 15, 30, 45 and 60 minutes after the injection of [^{11}C]RGH-1756 in three experiments. Fractions of radioactivity in the monkey plasma that corresponded to unchanged [^{11}C]RGH-1756 and labelled metabolites were determined using a modification of an HPLC-method previously developed for other PET ligands (Halldin et al. 1995). The radioactivity peaks in the HPLC chromatograms corresponding to either RGH-1756 or its labelled metabolites were integrated separately, and the areas were expressed as percentage of the sum of areas of all detected peaks.

In the second study the effect of reserpine induced DA depletion was examined on the binding of [^{11}C]RGH-1756 (Paper III). The monkeys were examined with [^{11}C]RGH-1756 two times on separate experimental days. On the first experimental day a baseline measurement was performed. Twenty-four hours before the second PET examination, each monkey received an intravenous injection of reserpine (0.5 mg/kg).

3.4.3. Examinations with [^{11}C]FLB 457 and [^{11}C]raclopride

Examination of the nine healthy comparison subjects was performed in the frame of an ongoing clinical study (Papers IV and V). All subjects were examined with [^{11}C]FLB 457 and [^{11}C]raclopride and underwent MR examination. A plastic helmet was made for each subject and used with a head fixation system to prevent head movements during the examinations (Bergstrom et al. 1981). The injected radioactivity was 151-265 MBq and 192-202 MBq in the examinations with [^{11}C]FLB 457 and [^{11}C]raclopride, respectively. Radioactivity in the brain was recorded in a series of consecutive time frames (3x1, 4x3, 12x6 min) over 87 min for [^{11}C]FLB 457, and (3x1, 4x3, 6x6 min) over 51 min for [^{11}C]raclopride.

To obtain high-resolution anatomical correlates for the PET images the subjects were examined using magnetic resonance imaging (1.5T, GE Signa MRI system, Milwaukee, WI). A T1w protocol (3D-SPGR, TR=20 msec, TE=5 msec, flip angle=35^{o}) was used to acquire 156 axial slices with 1 mm slice thickness. The field of view was 26 cm. The image matrix was 256x256, which yielded a voxel size of 1.02x1.02x1.00 mm.

3.5. IMAGE ANALYSIS, CALCULATIONS AND STATISTICS

3.5.1. [^{35}S]GTPγS binding autoradiography

The autoradiograms were digitized using a ScanMaker E6 high-resolution scanner (Mikrotek). Measurements and image processing were performed using Adobe Photoshop 6.0 and Matlab 6.5. To quantify [^{35}S]GTPγS binding the optical density values were transformed into units of nCi/mg tissue using ^{14}C-calibration scales (American Radiolabeled Chemicals Inc, St Louis, MO, USA).

Agonist stimulated binding in brain sections was expressed as the percentage increase in [^{35}S]GTPγS binding induced by the agonist relative to that observed under basal (agonist-free) conditions. Results of multiple measurements in the same region were averaged for each subject. These values were then used to calculate the mean agonist stimulated [^{35}S]GTPγS binding of the entire group. Standard error of mean (SEM) was calculated from the inter-individual variance and the number of subjects (Paper I).

3.5.2. PET studies with [^{11}C]RGH-1756

3.5.2.1. Image processing

All PET images obtained in the initial evaluation of [^{11}C]RGH-1756 (Paper II) were co-registered to the MR image of the same monkey using the Karolinska Computerized Brain Atlas System (Roland et al. 1994).

Each PET image obtained in the examination after administration of reserpine (Paper III) was co-registered to the baseline PET image of the same monkeys using a manual, image-overlay based technique (MARS, Willendrup et al. 2004).

3.5.2.2. Delineation of regions of interest

The uptake of [^{11}C]RGH-1756 was measured in more regions of the monkey brain during the initial evaluation of the radioligand (Paper II) than in the study that examined the effect of reserpine on the binding of [^{11}C]RGH-1756 (Paper III).

In the first PET study the uptake of [^{11}C]RGH-1756 was examined in several regions throughout the entire monkey brain (Paper II). The regions of interest (ROIs) were drawn on the MR image of the monkey, and were thereafter transferred to the PET images to measure the regional radioactivity concentration. ROIs for accumbens, caudate, putamen, hippocam-

pus, mesencephalon, thalamus, cingulate gyrus, cerebellar hemispheres, frontal and temporal cortices and the whole brain were delineated using the atlas of Paxinos & Toga (Paxinos, 2000).

In the PET studies with reserpine (Paper III) the uptake of [^{11}C]RGH-1756 was examined in the ventral striatum (ROI corresponding to the accumbens), dorsal striatum (ROI encompassing the putamen) and the cerebellum (lobules 9-10 were not included in the ROI). ROIs were drawn on the summation PET images from the baseline examinations, which represent radioactivity concentration measured between 9-93 min. Delineation of the ROIs was guided by an atlas of a cryosectioned Cynomolgus monkey brain *in situ* (Karlsson et al. 1993).

3.5.2.3. Quantification of [^{11}C]RGH-1756 binding in the monkey brain

The ROIs were used thereafter to measure total radioactivity concentration ($C_{T(t)}$, nCi/ml) in selected regions of the monkey brain. The time curve for $C_{T(t)}$ was plotted versus time for each ROI. A triple-exponential function was fitted to the TACs to reduce the noise at single time points. The TACs were normalized to the injected radioactivity. Non-specific binding ($C_{N(t)}$) was estimated from the radioactivity concentration measured in the cerebellar hemispheres, as this structure contains negligible amounts of D_3 receptors (Bancroft et al. 1998; Levant, 1998; Levesque et al. 1992; Ricci et al. 1995). Specific binding ($C_{B(t)}$) was calculated for each ROI as the difference between the total and non-specific binding. Binding potential (BP) was estimated as the ratio of specific to non-specific binding. In the initial PET study with [^{11}C]RGH-1756 (Paper II), the C_B and C_N measured at the time of peak equilibrium, i.e when dCb/dt=0 (Farde et al. 1989), was used to calculate BP. In the PET study that examined the effect of reserpine on [^{11}C]RGH-1756 binding (Paper III) the TACs for cerebellum and for specific binding in each ROI were integrated for the time period of 9-45 min for the calculation of BP:

$$BP = \int_{9}^{45} C_{B(t)}dt \,/\, \int_{9}^{45} C_{N(t)}dt$$

The two approaches for the calculation of BP yielded similar results.

An attempt was made to perform a Scatchard analysis based on the results of the initial PET examinations with [^{11}C]RGH-1756 performed in the same monkey (Paper II). Values of $C_{B(t)}$ and $C_{N(t)}$ obtained at the time of equilibrium were divided by the SA of [^{11}C]RGH-1756 to calculate the concentration of specifically bound (B; fmol/ml) and that of free (F; fmol/ml) radioligand. Scatchard analysis was performed using B and F values obtained from the experiments with varying injected mass of the RGH-1756, as described earlier (Farde et al. 1997; Ginovart et al. 1997). The density of [^{11}C]RGH-1756 binding sites (B_{max}) and apparent affinity of the ligand (K_d) were obtained from the Scatchard plot.

3.5.3. PET studies with [^{11}C]FLB 457 and [^{11}C]raclopride

3.5.3.1. Image processing

The MR images were segmented using the Bayesian probabilistic approach implemented in SPM2 (Ashburner & Friston, 1997). The original MR and the probability maps of gray matter (GM), white matter (WM), cerebrospinal fluid (CSF) and skull were thereafter co-registered to the PET image of the same subject using mutual information cost function (Maes et al. 1997) in SPM2 (Papers IV and V).

3.5.3.2. Delineation of regions of interest

ROIs were defined to obtain regional TACs for [^{11}C]FLB 457 and [^{11}C]raclopride binding (Papers IV and V). ROIs for striatum, thalamus, hippocampus, amygdala, anterior cingulate and insular cortex were delineated manually on the high-resolution T1w MR images. Segmentation of these regions and delineation of subregions within the thalamus and the striatum followed published anatomical recommendations. For the segmentation of the insular cortex, the methods of Crespo-Facorro et al. (2000) and of Kasai et al. (2003) were adapted. Anterior cingulate was delineated according to Ballamier et al. (2004), whereas hippocampus and amygdala were segmented following the guidelines of Pruessner et al. (2000).

Segmentation of the thalamus and its subregions was slightly modified as compared to the original recommendation of Buchsbaum et al. (1996) and that of Gilbert et al. (2001). Originally the inferior border of the third ventricle was proposed as the inferior boundary of the thalamus. Our approach was, in contrast, to use the rostral end of the superior colliculi as the inferior boundary of the thalamus, in order to reduce inter-rater differences in segmentation. According to the method of Gilbert et al. (2001) the thalamus is subdivided into five small regions (Figure 8A). Some of these thalamic subregions were, however, so small that statistical noise at late time points of the TACs prevented quantitative analysis of [^{11}C]FLB 457 binding in these regions. According to previous PET studies with [^{11}C]FLB 457 (Yasuno et al. 2004) and in vitro autoradiographic studies (Hall et al. 1996a; Rieck et al. 2004) the density of D_2 receptors is similar in the anterior and central medial thalamic subdivisions. The same principal applies to the anterior and central lateral subdivisions. Therefore only three thalamic subregions were defined for the full quantitative analysis: medial, lateral and posterior. The ventral striatum, the dorsal part of caudate and the dorsal part of putamen (Figure 8B) were delineated according to the method of Mawlawi et al. (2001) and Martinez et al. (2003).

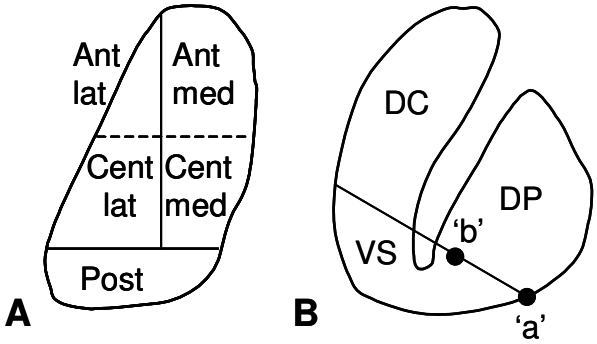

Figure 8. *Delineation of subregions in the thalamus (***A***) and the striatum (***B***). Gilbert et al. (2001) defined 5 subregions in the thalamus. In the present study anterior and central subregions were merged on both lateral and medial side of the thalamus. Striatum was subdivided into 3 subregions according to Mawlawi et al. (2001): ventral striatum (VS), dorsal part of caudate (DC) and dorsal part of putamen (DP). Point 'a' is the intersection of the lateral border of the putamen and a vertical line going through the most superior and lateral point of the capsula interna. Point 'b' is the middle of the part of the AC plane that falls within the striatum.*

Manual segmentation of the regions was performed using MRICro (Rorden & Brett, 2000). The ROIs were then re-sliced using the corresponding transformation matrix obtained during the co-registration of the MR image to the PET image of the same subject. The re-sliced ROIs were transferred to the PET images to obtain the regional TACs of [^{11}C]FLB 457 and [^{11}C]raclopride before PVE correction.

An automated ROI fitting algorithm was used to define ROIs for frontal, parietal, temporal and occipital cortices, subtentorial GM, WM and CSF. The automated method is based on the coordinate system of the Talairach atlas (Talairach & Tournoux, 1988), as described previously in detail (Andreasen et al. 1996; Quarantelli et al. 2002).

3.5.3.3. Partial volume effect correction

PVE correction was performed using an ROI based method proposed by Rousset et al (1998a), which accounts for spill-in and spill-out effects between any possible pair of ROIs (Papers IV and V). This method was shown to be as effective and accurate as established, pixel-based methods (Muller-Gartner et al. 1992) in recovering activity loss due to PVE. Moreover, this method provided more consistent estimates when applied to real data, and did not require any *a priori* knowledge of regional tracer levels, as was the case for pixel-based methods (Rousset et al. 1998b).

Briefly, uncorrected TACs were first obtained by applying the complete ROI set (manually and automatically segmented GM ROIs, plus two additional ROIs for the WM and the CSF compartments) to the PET images. Then a matrix of regional transfer coefficients was calculated for the same ROI set, based on the known resolution of the PET images. The transfer coefficient (ω_{ij}) represents the fraction of activity transferred from ROI_i to ROI_j because of PVE, and is derived as follows.

$$\omega_{ij} = \frac{1}{n_{pix}} \int_{ROI_j} RSF_i(r)dr$$

where n_{vox} is the number of voxels in ROI_j, $RSF_i(r)$ represents the regional spread function of ROI_i, and is calculated by integration of the system's PSF over ROI_i, and r is a three dimensional vector in the image space. The original PET values and the transfer coefficients compose a system of linear equations, the unknowns being the true mean ROI values. In general form for N number of ROIs:

$$t_j = \sum_{i=1}^{N} \omega_{ij} T_i$$

where t represents the observed and T the PVE corrected (True) activity concentration in the ROIs. The system of linear equations is solved inverting the matrix of regional transfer coefficients by Single Value Decomposition, thus providing the PVE corrected ROI values. In the matrix inversion process, activity in CSF is forced to zero to increase accuracy by taking advantage of the *a priori* knowledge of the lack of appreciable activity in CSF (Quarantelli et al. 2004). Regional recovery coefficients (RC), that are for each ROI the ratio of observed to true activity in the absence of surrounding activity (Hoffman et al. 1979, 1982) represent the diagonal of the transfer matrix. The algorithm for PVE correction was implemented in a common software framework (Quarantelli et al. 2004; Rask et al. 2004).

3.5.3.4. Quantification of [^{11}C]FLB 457 and [^{11}C]raclopride binding in brain

The same approach was used for the quantification of radioligand binding for [^{11}C]FLB 457 and [^{11}C]raclopride (Papers IV and V). The standard two tissue compartment model (2-TCM, Figure 9) with estimated arterial input functions was used for kinetic analysis of radioligand binding before and after PVE correction. This model was proven to be useful for the quantification of both [^{11}C]FLB 457 and [^{11}C]raclopride binding to D_2/D_3 receptors (Endres et al. 1997; Farde et al. 1986, 1989; Lammertsma et al. 1996; Olsson et al. 1999). The four rate constants (K_1, k_2, k_3 and k_4) were estimated by standard nonlinear least–squares analysis using the Marquardt algorithm (Marquardt, 1963). Cerebral blood volume was set as 5% for all ROIs (Yamaguchi et al. 1986). Binding potential (BP, Mintun et al. 1984) and total distribution volume (DV_{tot}) were calculated in the following way: $BP=k_3/k_4$, $DV_{tot}=K_1/k_2(1+k_3/k_4)$.

As no arterial blood samples were taken from this set of comparison subjects during the PET examinations, the input functions for [^{11}C]FLB 457 and [^{11}C]raclopride were estimated according to previously published experimental data (Endres et al. 1997; Farde et

al. 1986, 1989; Lammertsma et al. 1996; Olsson et al. 1999, 2004) and measurements performed earlier in our laboratory (unpublished observations).

To allow for the comparison of radioligand binding before and following PVE correction, the arterial plasma and blood curves were estimated as follows. The overall strategy for the generation of the simulated arterial curves was to find an arterial curve for each subject that provided binding parameters consistent with the results of the simplified reference tissue model (SRTM, Lammertsma & Hume, 1996). It has previously been demonstrated that BP values of [^{11}C]FLB 457 and that of [^{11}C]raclopride obtained with SRTM and 2-TCM are in good agreement (Lammertsma et al. 1996; Olsson et al. 1999, 2004).

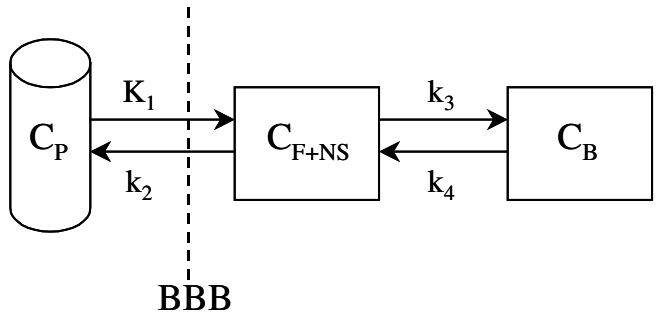

Figure 9. *Schematic delineation of the standard two-tissue compartment model. C_P represents the arterial input function, whereas C_{F+NS} and C_B indicate tissue compartments of free+non-specifically bound and specifically bound ligand, respectively. The exchange rate of the ligand between compartments is described by four rate constants, K_1-k_4. BBB, blood-brain barrier*

In the first phase of the analysis SRTM was used to calculate BP and R1 ($R1=K_1/K_1'$, where K_1' is the influx rate constant of the reference region) before PVE correction for [^{11}C]FLB 457 and [^{11}C]raclopride. Cerebellum was used as reference region, as it contains negligible amounts of D_2/D_3 receptors (Camps et al. 1989; Camus et al. 1986; De Keyser et al. 1988; Hall et al. 1994, 1996a; Olsson et al. 1999).

In the following step of the analysis the 2-TCM was fit to the non-PVE corrected (henceforth observed) TACs of [^{11}C]FLB 457 and [^{11}C]raclopride in each subject using several different simulated plasma and whole blood curves. For [^{11}C]raclopride the single-tissue compartment model was used for the cerebellum to obtain K_1', as the 2-TCM did not reach convergence for this region. BP and R1 were then also calculated using the rate constants obtained from the 2-TCM.

The plasma curve and the corresponding blood curve, which resulted in parameters that were in best agreement with results of the SRTM, were selected for further analysis for each subject. The agreement between BP and R1 values calculated with 2-TCM and SRTM was assessed using intra-class correlation coefficient ($ICC_{3,1}$) according to the definition of Schrout & Fleiss (1979). For [^{11}C]FLB 457 $ICC_{3,1}\geq0.72$ for R1 and $ICC_{3,1}\geq0.73$ for BP, whereas for [^{11}C]raclopride $ICC_{3,1}\geq0.72$ for R1 and $ICC_{3,1}\geq0.40$ for BP in each subject (Table 4). Furthermore, the simulated plasma curves were adjusted so that the rate constants were within the previously published, physiological range (Endres et al. 1997; Farde et al. 1986, 1989; Lammertsma et al. 1996; Olsson et al. 1999, 2004).

3.5.3.5. Statistical analysis

Analysis of PVE correction induced changes in rate constants, BP and DV_{tot} of [^{11}C]FLB 457 (Paper IV) was performed using analysis of variance for repeated-measures (ANOVA, general linear model module, Statistica 7.1, StatSoft, Tulsa, OK). For [^{11}C]raclopride the multivariate approach was used (Paper V). Each parameter was tested for two between subject effects. The first main effect reflected the overall change of parameters after PVE correction, whereas the other main effect referred to the difference of parameters between

distinct brain regions. The interaction of these two main effects was also examined. Significance level was set at $\alpha<0.05$. For the ANOVA approach ([^{11}C]FLB 457, Paper IV) Mauchly's test of sphericity was used to examine whether the sphericity assumption was fulfilled, and the correction method of Huynh & Feldt was used whenever it was violated (Huynh & Feldt, 1976). The Cook's distance was used to detect outliers.

If the ANOVA indicated significant interaction effect, planned comparisons were performed with Bonferroni correction to test the difference of observed and PVE corrected values in each ROI.

Pearson's R was calculated to examine the relationship of ROI volumes to regional RC values and to changes of binding parameters (BP and DV_{tot}) of both radioligands following PVE correction. Bonferroni correction was applied to detect significant correlations. Significance level was set at $\alpha<0.05$.

	BP		**R1**	
	2-TCM	**SRTM**	**2-TCM**	**SRTM**
Ventral striatum	1.6 ± 0.4	2.0 ± 0.2	1.11 ± 0.21	0.93 ± 0.07
Dorsal caudate	2.1 ± 0.3	2.1 ± 0.2	0.98 ± 0.17	0.83 ± 0.04
Dorsal putamen	2.3 ± 0.3	2.9 ± 0.2	1.28 ± 0.20	1.05 ± 0.06
Med. thalamus	2.2 ± 0.4	2.8 ± 0.6	1.11 ± 0.07	1.09 ± 0.07
Post. thalamus	1.9 ± 0.4	2.0 ± 0.6	0.98 ± 0.11	0.99 ± 0.08
Lat. thalamus	1.5 ± 0.3	1.6 ± 0.4	1.01 ± 0.06	1.02 ± 0.04
Hippocampal compl.	1.3 ± 0.4	0.9 ± 0.3	0.85 ± 0.04	0.86 ± 0.05
Insula	1.2 ± 0.2	1.0 ± 0.3	1.03 ± 0.03	1.00 ± 0.04
Ant. cingulate	0.8 ± 0.2	0.5 ± 0.2	1.03 ± 0.05	1.01 ± 0.05
Temporal cx.	1.0 ± 0.2	0.7 ± 0.2	0.93 ± 0.04	0.93 ± 0.03
Frontal cx.	0.6 ± 0.1	0.3 ± 0.2	1.02 ± 0.05	1.00 ± 0.04
Parietal cx.	0.6 ± 0.2	0.3 ± 0.2	1.02 ± 0.05	0.99 ± 0.05
Occipital cx.	0.5 ± 0.2	0.3 ± 0.2	1.09 ± 0.06	1.06 ± 0.04

Table 4. *BP and R1 values calculated using 2-TCM and SRTM. [^{11}C]raclopride was used to examine the striatum and [^{11}C]FLB 457 was used for all other regions. The data shows the mean ± SD of results obtained in nine and eight subject for [^{11}C]FLB 457 and for [^{11}C]raclopride, respectively. The 2-TCM columns show the average of those parameters for each subject that was obtained using the individually optimized plasma curves.*

4. RESULTS AND COMMENTS

4.1. AUTORADIOGRAPHIC MAPPING OF DOPAMINE-D_2/D_3 RECEPTOR STIMULATED [^{35}S]GTPγS BINDING IN THE HUMAN BRAIN (PAPER I)

Agonist stimulated [^{35}S]GTPγS binding autoradiography had earlier been successfully applied for the examination of D_2/D_3 receptors in the rat brain (Culm et al. 2003; Febo et al. 2003; He et al. 2000; Newman-Tancredi et al. 2001). DA, quinelorane and quinpirole, but not SKF-238393, a D_1 agonist stimulated [^{35}S]GTPγS binding in the striatum and the cingulate cortex of the rat brain. Previously agonist stimulated [^{35}S]GTPγS binding autoradiography has not been applied for the examination of DA receptors in human brain sections.

The objectives of the present study were to establish agonist stimulated [^{35}S]GTPγS binding autoradiography for the examination of DA receptors in whole human hemisphere sections, and to describe the distribution of dopamine-D_2/D_3 receptor activated G proteins.

4.1.1. Optimisation studies

In previous experiments examining agonist stimulated [^{35}S]GTPγS binding at DA receptors in rat brain sections, the assay conditions were almost the same as originally proposed by Sim et al. (1995). The procedure involved two preincubations without agonist (15 min each, in 50mM Tris-HCl buffer, pH 7.4, supplemented with 100 mM NaCl, 3 mM $MgCl_2$, 0.2 mM EGTA and 2 mM GDP for the second preincubation only), which were followed by an incubation of 1-2 h in the same buffer with the addition of [^{35}S]GTPγS and an agonist. The assay was usually performed at room temperature.

No stimulation of [^{35}S]GTPγS binding was observed on DA receptors in human brain sections by application of the assay condition used to examine rat brain. Therefore, the optimisation of assay conditions was first necessary for the measurement of DA stimulated [^{35}S]GTPγS binding in human brain sections. The optimisation procedure generally involves varying the incubation time and temperature, modifying the concentration of GDP, magnesium, sodium and changing the buffering agent. In the present optimisation studies, however, no DA stimulated [^{35}S]GTPγS binding was observed in human brain sections by changing the incubation temperature, lengthening the incubation time or by modifying the concentration of GDP, magnesium or the type of buffer used. Changes to the concentration of sodium in the incubation buffer needed careful consideration. As it has been shown that high Na^+ concentration shifts DA receptors to low affinity state (Grigoriadis & Seeman, 1985; Kapur & Seeman, 2001; Watanabe et al. 1985), increasing the concentration of Na^+ in the incubation solution might inhibit DA receptor activation. On the other hand increasing the concentration of monovalent salts in the incubation buffer could be beneficial for the reduction of basal binding (Happe et al. 2001; Sim et al. 1995), which was rather high in the 100 μm thick human brain sections. Considering the advantageous and disadvantageous effects of increasing the concentration of monovalent salts in the incubation buffer, we

Na^+ (mM)	K^+ (mM)	Basal binding (nCi/mg tissue)	Stimulation by DA (% above basal)
100	50	1.4 ± 0.4	24.1 ± 5.6
150	75	1.2 ± 0.0	26.7 ± 12.7
200	100	0.6 ± 0.0	21.6 ± 12.7

Table 5. *The effect of different concentrations of monovalent salts on basal and DA (1 mM) stimulated [^{35}S]GTPγS binding in the striatum in human brain section. Mean ± SEM is presented, number of subjects examined: n =2.*

tested the effect of keeping the original sodium concentration (100 mM) and adding potassium (50 mM) to the incubation buffer. We also hypothesized that the mixture of sodium and potassium in the incubation buffer would mimic the composition of both the intra- and the extracellular compartment, and thereby promote that conformation of DA receptors and G proteins, which is present in the brain under physiological conditions. Indeed, after modifying the concentration of monovalent salts in the incubation buffer DA stimulated [^{35}S]GTPγS binding was detected in the striatum in human brain sections at room temperature (9.5 ± 2.1 %, mean ± SEM, number of subjects = 2 for all results obtained in the optimisation procedure). DA stimulated [^{35}S]GTPγS binding was even higher when the incubation was performed at 37 °C (24.1 ± 5.6 %; Table 5). Thereafter, the effect of different concentrations of sodium and potassium was examined on basal and DA stimulated [^{35}S]GTPγS binding (Table 5). Similar to previous results (Happe et al. 2001; Hilf et al. 1989; Sim et al. 1995), a progressive decrease in basal binding was detected by increasing the concentration of monovalent salts. At very high salt concentrations (300 mM) a tendency for lower DA stimulated binding was observed, probably due to the aforementioned effect of sodium on the affinity-state of dopamine receptors (Grigoriadis & Seeman, 1985; Kapur & Seeman, 2001; Watanabe et al. 1985). Therefore the mixture of 150 mM NaCl and 75 mM KCl was used afterwards. The incubation time was set to 90 min in order to avoid substantial damage to the tissue sections.

4.1.2. Characterisation of agonist stimulated [^{35}S]GTPγS binding at D_2/D_3 receptors in the human brain

Basal [^{35}S]GTPγS binding was heterogeneous in the brain, and was highest in striatum, frontal and insular cortices and the medial part of thalamus. In comparison with the basal condition, addition of DA resulted in increased [^{35}S]GTPγS binding in several brain areas, including striatum, SN, thalamus and hippocampus (Table 6).

Raclopride, a D_2/D_3-selective antagonist potently inhibited the stimulatory effect of DA on [^{35}S]GTPγS binding in the striatum and the hippocampus, whereas SCH23390 did not diminish DA stimulated [^{35}S]GTPγS binding in any regions. This observation indicates that DA induced [^{35}S]GTPγS binding is mediated primarily by D_2/D_3 receptors, and the involvement of D_1 receptors in the present assay is unlikely. This is in line with the generally accepted suggestion that agonist stimulated [^{35}S]GTPγS binding autoradiography is suitable for the examination of G_i/G_o, but not G_s coupled receptors (Happe et al. 2001; Sim et al. 1995). However, in some regions, including the ventral part of caudate and putamen, hippocampus, SN, and some cortical regions, raclopride did not completely abolish DA stimulated [^{35}S]GTPγS binding. It is possible that DA stimulated [^{35}S]GTPγS binding at D_4 receptors, as this receptor subtype is present in these brain areas (Lahti et al. 1995;

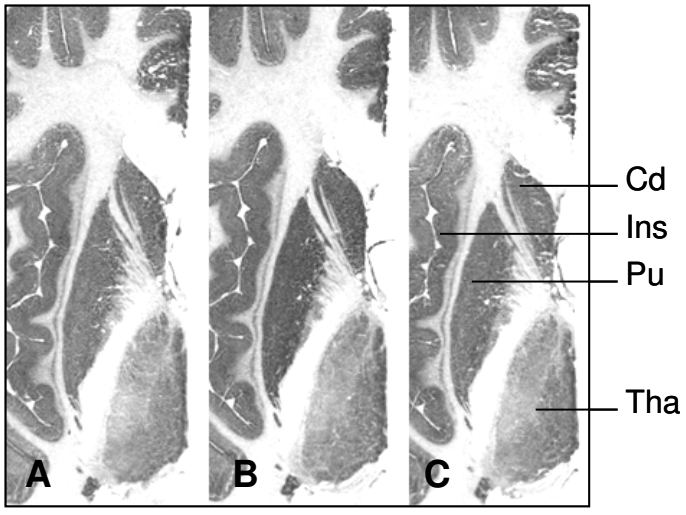

Figure 10. *[^{35}S]GTPγS binding in the human striatum.* **A.** *Basal binding.* **B.** *DA (1 mM) stimulated binding.* **C.** *DA stimulated [^{35}S]GTPγS binding blocked by raclopride (0.1 mM). Cd, caudate; Ins, insula; Pu, putamen; Tha, thalamus.*

Primus et al. 1997). However, to verify the possible role of D_4 receptors in stimulating [^{35}S]GTPγS binding in human brain sections, it is necessary to use a selective and highly potent agonists at the D_4 receptor.

	DA (1 mM)				DA (1 mM) and Raclopride (0.1 mM)				Quinpirole (1 mM)			
	mean	SEM	n	N	mean	SEM.	n	N	mean	SEM.	n	N
Putamen	23.0	2.3	3	13	3.0*	0.8	3	7	16.3	6.0	3	6
dorsal put.	31.0	1.9	3	6	-4.5	5.8	2	2	20.9	8.8	3	3
ventral put.	15.7	4.5	3	7	6.0*	1.4	3	5	11.7	3.5	3	3
Caudate	20.2	0.3	3	13	0.8*	1.1	3	7	16.6	3.3	3	6
dorsal caud.	24.4	1.6	3	6	-11.7	6.5	2	2	23.8	4.9	3	3
ventral caud.	15.2	3.1	3	7	6.8	3.9	3	5	9.4	3.0	3	3
Subst. nigra	22.3	1.6	2	4	6.6	0.6	2	3	12.8	5.8	3	3
Amygdala	17.3	7.5	2	3	9.6	8.6	2	3	4.3	1.4	2	2
Hippocampus	15.7	6.0	3	6	4.3*	0.9	3	6	8.5	2.4	4	6
Ant. cingulate	12.7	1.8	3	11	4.7	5.4	3	4	8.9	5.1	3	6
Thalamus	11.9	2.0	3	6	1.1	0.9	2	2	9.6	6.3	3	5
Insular cx.	4.5	1.7	3	12	-0.2	2.3	3	6	5.5	2.2	3	5
Temporal cx.	4.4	3.2	3	15	4.4	5.1	3	8	1.7	2.1	4	8
Occipital cx.	3.7	1.4	3	11	1.7	1.1	3	6	1.3	1.5	4	8
Frontal cx.	3.6	1.0	3	14	0.4	1.9	3	9	2.3	0.5	4	9
Pallidum	1.8	6.6	3	7	5.0	6.7	3	5	4.3	5.1	3	3

Table 6. *DA and quinpirole stimulated [^{35}S]GTPγS binding in whole human hemisphere sections, and the effect of raclopride on DA stimulated binding. Data are presented as % stimulation above basal. *, significant difference compared to DA stimulated binding, Mann-Whitney U test ($p<0.05$); n, number of subjects; N, total number of sections studied. From Paper I.*

The highest DA stimulated [^{35}S]GTPγS binding was measured in the striatum (Figure 10). Within the striatum the level of DA stimulated [^{35}S]GTPγS binding was heterogeneous. Statistical analysis (two-way ANOVA) revealed that DA stimulated [^{35}S]GTPγS binding was significantly higher in the dorsal than in the ventral parts of caudate and putamen. Previous studies using traditional radioligand autoradiography demonstrated no dorsoventral gradient in the density of D_2 receptors within in the striatum (Camus et al. 1986; Hall et al. 1994; Piggott et al. 1999). In contrast, the density of D_3 receptors is much higher in the ventral striatum, including the nucleus accumbens than in the dorsal part (Hall et al. 1996b; Murray et al. 1994). In this study, DA stimulated [^{35}S]GTPγS binding was not examined in the nucleus accumbens. However, the lower stimulation in the ventral part of the striatum could be due to low or no stimulation at D_3 receptors, as it is known that dopamine-D_3 receptors are only weakly coupled to G proteins (Chio et al. 1994; Newman-Tancredi et al. 1999; Vanhauwe et

al. 1999). The dorsal and the ventral parts of the striatum are viewed as two functionally distinct compartments, with different input and output connections (Kunzle, 1975, 1977; Selemon & Goldman-Rakic, 1985) and different characteristics of dopaminergic neurotransmission (Cragg et al. 2000, 2002). The dorsal part is involved in the regulation of motor function, whereas the ventral part mediates emotional and motivational processes. The observed difference of D_2 receptor induced G protein activation between ventral and dorsal parts of caudate and putamen might reflect the distinct functional role and DA transmission pattern of these receptors.

The level of DA stimulated [^{35}S]GTPγS binding detected in the SN (22%, Figure 11) was almost as high as levels detected in the striatum, despite that the density of D_2 receptors in the SN is less than one-fourth of the striatal density (Hall et al. 1994). The D_2-like receptors in the SN are somatodendritic autoreceptors, whereas in other regions D_2 receptors are located both postsynaptically and presynaptically (for more reviews see Elsworth & Roth, 1997). It has been suggested that DA autoreceptors are more sensitive to the effects of DA than heteroceptors (Carlsson et al. 2004; Elsworth & Roth, 1997). The more efficient coupling of DA receptors and G proteins in the SN could contribute to the higher responsiveness of autoreceptors.

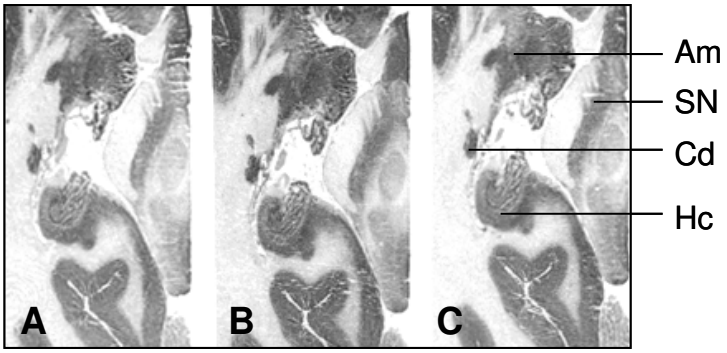

Figure 11. *[^{35}S]GTPγS binding in the human brain at the level of the substantia nigra.* **A.** *Basal binding.* **B.** *DA (1 mM) stimulated binding.* **C.** *DA stimulated [^{35}S]GTPγS binding blocked by raclopride (0.1 mM). Am, amygdala, SN, substantia nigra; Cd, caudate; Hc, hippocampus.*

Relatively high levels of DA stimulated [^{35}S]GTPγS binding were detected in thalamus and in some limbic brain regions, including amygdala, hippocampus and anterior cingulate, although these regions contain low or very low densities of D_2-like receptors. The higher stimulation could therefore reflect regional differences in the efficiency of DA receptor/G protein coupling.

The distribution of quinpirole stimulated [^{35}S]GTPγS binding was similar to that of DA stimulated. The highest quinpirole stimulated binding was measured in striatum, followed by SN, whereas moderate levels of stimulation were detected in hippocampus, thalamus, anterior cingulate and amygdala. Quinpirole stimulated [^{35}S]GTPγS binding was numerically lower than DA stimulated binding. However, no statistically significant differences have been observed between the level of DA and quinpirole stimulated [^{35}S]GTPγS binding (Table 6). Quinpirole, like DA, stimulated [^{35}S]GTPγS binding to a somewhat higher level in the dorsal than in the ventral parts of caudate and putamen. Statistical analysis revealed a pronounced tendency for higher stimulation in the dorsal parts.

In the present study agonist stimulated [^{35}S]GTPγS binding autoradiography was established to examine DA receptors in the human brain. The results demonstrate that this novel method could be a suitable technique for the examination of dopamine-D_2/D_3 receptors in the *postmortem* human brain, by providing useful new information about DA receptor/G protein coupling.

4.2. EVALUATION OF THE PUTATIVE DOPAMINE-D_3 SELECTIVE LIGAND, [^{11}C]RGH-1756 IN THE MONKEY BRAIN WITH PET (PAPERS II AND III)

In vitro examination of the D_3 receptors has been performed already using D_3-preferring radioligands, like [^{3}H]PD 128907 and [^{3}H]7-OH-DPAT, which also possess some affinity for D_2 receptors (Table 3). No successful *in vivo* labelling of D_3 receptors has yet been performed, and currently there are no selective radioligands available for the examination of D_3 receptors with PET.

The novel phenoxyalkylpiperazine derivative, RGH-1756, has about one-hundred times higher affinity for D_3 than for D_2 receptors (Laszlovszky et al. 2000). This indicates a higher selectivity of RGH-1756 for D_3 receptor than that of known D_3-preferring ligands, such as PD 128907 and 7-OH-DPAT. These properties of RGH-1756 render the molecule a promising candidate for *in vitro* and *in vivo* imaging of the dopamine-D_3 receptors in the brain. Recent successful radiolabelling of the molecule with carbon-11 (Langer et al. 2000) makes it possible to examine the potential of [^{11}C]RGH-1756 as a radioligand for PET.

	Low mass	High mass	unlabelled RGH-1756	Raclopride	WAY-100635
SA (GBq/µmol)	71.3	56.3	58.2	57.4	51.8
Inj. mass (µg)	0.17	0.41	0.14	0.42	0.18
Accumbens	0.32	0.29	0.13	0.17	0.33
Caudate	0.26	0.17	0.01	0.05	0.16
Putamen	0.43	0.36	0.04	0.26	0.32
Mesencephalon	0.20	0.22	0.01	0.12	0.18
Hippocampus	0.24	0.20	0.01	0.23	0.22
Thalamus	0.32	0.25	0.11	0.22	0.21
Frontal cx.	0.17	0.22	0.04	0.05	0.23
Temporal cx.	0.37	0.31	0.40	0.27	0.38
Ant. cingulate	0.32	0.29	0.33	0.17	0.35

Table 7. *BP of [^{11}C]RGH-1756 in selected regions of the monkey brain. The results were obtained in a baseline examination (low mass column), in an examination with high injected mass of unlabelled RGH-1756 (high mass column) and in pretreatment examinations with one of the following compounds: unlabelled RGH-1756 (0.02 mg/kg), raclopride (1 mg/kg) or WAY-100635 (0.5 mg/kg). BP was calculated as the ratio of specific to nonspecific binding at the time of peak equilibrium.*

4.2.1. Characterisation of [^{11}C]RGH-1756 binding in the monkey brain with PET (Paper II)

One cynomolgus monkey was repeatedly examined with [^{11}C]RGH-1756 in order to describe the distribution and specificity of [^{11}C]RGH-1756 binding in the monkey brain.

After iv injection of [^{11}C]RGH-1756, 1.0-1.1% of the total injected radioactivity was in the brain 30 seconds following the injection of the radioligand, which is rather low when compared to established radioligands, such as [^{11}C]raclopride (Halldin et al. 1991) or [^{11}C]FLB 457 (Halldin et al. 1995).

[^{11}C]RGH-1756 was homogenously distributed within the monkey brain, and no conspicuous accumulation of radioactivity could be seen by visual inspection of the PET images. BP of [^{11}C]RGH-1756 was low in all regions examined (Table 7). The highest values were measured in striatum, thalamus and temporal cortex. The inter-regional differences of BP were, however, small. The *in vitro* density of D_3 receptor is highest in the islands of Calleja and the nucleus accumbens (Bancroft et al. 1998; Levesque et al. 1992). The islands of Calleja are too small to be detected with PET, so this region was not analyzed in the present study. Nucleus accumbens did not stand out as having particularly high [^{11}C]RGH-1756 binding. The relative regional distribution of [^{11}C]RGH-1756 binding was thus not fully consistent with the rank order of regional D_3 receptor densities predicted by in vitro studies (Bancroft et al. 1998; Levesque et al. 1992; Stanwood et al. 2000a).

Pretreatment experiments were used to characterize the specificity of [^{11}C]RGH-1756 binding. Pretreatment with unlabeled RGH-1756 resulted in decreased binding of the radioligand in all brain regions, except temporal cortex and cingulate gyrus. The effect of unlabelled RGH-1756 on the binding of [^{11}C]RGH-1756 indicates saturable binding in the monkey brain. Pretreatment with raclopride (1 mg/kg) diminished binding of [^{11}C]RGH-1756 in many areas, including accumbens, caudate, putamen, mesencephalon, and frontal cortex, suggesting that binding of [^{11}C]RGH-1756 may represent specific binding to D_2/D_3 receptors. Pretreatment with WAY-100635 (0.5 mg/kg) had no effect on the radioactivity concentration of [^{11}C]RGH-1756 in any brain areas. Thus, it can be rule out that [^{11}C]RGH-1756 binds to 5-HT_{1A} receptors *in vivo*.

Although BP of [^{11}C]RGH-1756 was generally low, the pretreatment experiments with unlabelled RGH-1756 and raclopride showed some specific binding to binding sites that are presumably D_2/D_3 receptors. Based on this assumption we made an attempt to measure the density of D_3 receptors in the monkey brain by varying the injected mass of RGH-1756. After injection of the radioligand with higher mass of the unlabelled compound BP of [^{11}C]RGH-1756 was somewhat lower in striatum, thalamus and temporal cortex. In these regions the injected mass of RGH-1756 was inversely related to the BP of [^{11}C]RGH-1756 (Figure 12). No effect of the injected mass of RGH-1756 on the BP of [^{11}C]RGH-1756 was observed in the other brain regions. Scatchard analysis was performed for the regions in which the inverse relationship between the BP of [^{11}C]RGH-1756 and the injected mass of RGH-1756 was observed. As BP values of [^{11}C]RGH-1756 obtained in the experiments with low and high injected mass were hardly different in any regions, data points of the Scatchard plots were situated close together. Therefore the results did not provide reliable measures of B_{max} of D_3 receptors. The most likely reasons for the unsuccessful Scatchard analysis were the low signal from [^{11}C]RGH-1756 binding and the small difference in the injected mass of RGH-1756 between the examinations.

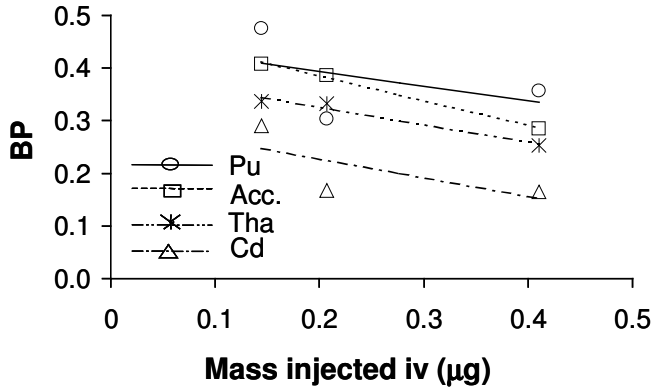

Figure 12. *Relationship between the injected mass of RGH-1756 and the BP of [^{11}C]RGH-1756. Correlation coefficient (R) in putamen (Pu) -0.43; accumbens (Acc) -0.99; thalamus (Tha) -0.98; caudate (Cd) -0.70 (from Paper II).*

The results of the present study do not demonstrate that [^{11}C]RGH-1756 is suitable for *in vivo* imaging of D_3 receptors. This

was somewhat unexpected, since RGH-1756 has promising *in vitro* binding characteristics. Common reasons for failures *in vivo* are low affinity under physiological conditions, high non-specific binding, and rapid degradation of the radiolabelled molecule. In the present study there was no support for high non-specific binding or unusually rapid metabolism, whereas it cannot be excluded that the affinity at *in vivo* conditions is not sufficient to visualize the minute densities of D_3 receptors in the brain.

With regard to imaging of D_3 receptors there is, however, another biological condition which has to be taken into account. *In vitro* radioligand binding studies suggested that D_3 receptors are occupied by DA to a high degree (Levesque et al. 1992; Schotte et al. 1992, 1996). This assumption gained further support by the observation that depletion of endogenous DA with reserpine and α-methyltyrosine increased the binding of [^{3}H]7-OH-DPAT in the rat brain in *ex vivo* autoradiographic experiments (Levant, 1995).

4.2.2. Examination of the effect of dopamine depletion on the binding of [^{11}C]RGH-1756 (Paper III)

Based on previous experimental data, it is possible that endogenous DA prevents *in vivo* binding of [^{11}C]RGH-1756 in the monkey brain. To challenge this assumption the effect of reserpine induced DA depletion on the binding of [^{11}C]RGH-1756 was examined in three monkeys.

Reserpine effectively decreases synaptic concentration of DA (Guo et al. 2003; Kuczenski, 1977; Stanwood et al. 2000b) by depletion of available stores of catecholamines. It inhibits catecholamine uptake into storage vesicles by the blockade of vesicular monoamine transporter proteins (Alvaro et al. 2001). Reserpine had frequently been used in PET studies to examine the effect of endogenous neurotransmitters on the binding of several radioligands, including [^{11}C]raclopride (Ginovart et al. 1997), [^{11}C]SCH23390 (Chou et al. 1999), [^{11}C]NPA (Cumming et al. 2002), [^{11}C]NNC 112 (Guo et al. 2003), [^{11}C]WAY-100635 (Maeda et al. 2001) and [^{11}C]PE2I (Poyot et al. 2001). The binding of the aforementioned radioligands was increased after the administration of reserpine, except for [^{11}C]PE2I, which showed lower binding following reserpine treatment and [^{11}C]WAY-100635, which was not influenced by reserpine.

In the present study the binding of [^{11}C]RGH-1756 was examined 24 hours after the administration of 0.5 mg/kg reserpine in the striatum in three monkeys, and the results were compared to baseline measurements of the same monkeys.

Results of the baseline measurements were in good agreement with results of the previous study with [^{11}C]RGH-1756. In the baseline measurements 1.0-1.5% of the injected radioactivity was in brain one minute after the administration of the [^{11}C]RGH-1756. Within the brain the regional distribution of [^{11}C]RGH-1756 was homogenous. Specific binding of [^{11}C]RGH-1756 was low and not different between the ventral and the dorsal striatum. Baseline BP values were low, and there were no evident regional differences of BP in any monkey (Table 8).

After administration of reserpine 1.0-1.2% of the injected radioactivity was in the brain. The peak value of whole brain uptake of [^{11}C]RGH-1756 was observed during the first minute of the examination, as for the baseline measurements. Reserpine caused no evident changes in the distribution of [^{11}C]RGH-1756 within the monkey brain, and no obvious regional accumulation of radioactivity could be seen by visual inspection of the PET images. Reserpine had no consistent effect on specific [^{11}C]RGH-1756 binding in the monkey brain. In the first and second monkey, specific [^{11}C]RGH-1756 binding decreased after the administration of reserpine both in ventral and dorsal striatum. The decrease was most pronounced during the first half of the PET measurements in both monkeys. In the third monkey, specific [^{11}C]RGH-1756 binding was slightly increased after the administration of

reserpine. The increase of specific [^{11}C]RGH-1756 binding was most evident during the first 20 minutes of the PET measurement. BP values of [^{11}C]RGH-1756 were low in all monkeys after the administration of reserpine, and no consistent changes of the regional BP values were observed when compared to the baseline values (Table 8).

After reserpine treatment there was no consistent increase in specific binding and BP of [^{11}C]RGH-1756 in the striatum of the monkeys. On the contrary, BP of [^{11}C]RGH-1756 was decreased in the striatum of two monkeys after administration of reserpine. This observation does not support the hypothesis that binding of [^{11}C]RGH-1756 to D_3 receptors in the monkey brain is inhibited by high occupancy of D_3 receptors by endogenous DA. Nevertheless, the results of the present study confirm the view from previous experiments that [^{11}C]RGH-1756 is not suitable for *in vivo* examination of D_3 receptors.

The signal obtained for possible specific binding of [^{11}C]RGH-1756 in the Cynomolgus monkeys' brains was low both in the baseline and the pretreatment measurements. Such low signal, as obtained for specific binding of [^{11}C]RGH-1756, can be confounded by noise to a high degree. In our case, this low signal to noise ratio may explain the inconsistency in reserpine induced changes of specific [^{11}C]RGH-1756 binding in the three monkeys.

Results of the present examinations, together with results of the previous study (Paper II) demonstrate that the cause of low specific binding of [^{11}C]RGH-1756 is the insufficient *in vivo* affinity of the ligand for D_3 receptors, and not high occupancy of D_3 receptors by endogenous DA. Despite the promising *in vitro* results [^{11}C]RGH-1756 was not suitable for PET imaging of D_3 receptors.

	Monkey 1		Monkey 2		Monkey 3	
	Baseline	**Reserpine**	**Baseline**	**Reserpine**	**Baseline**	**Reserpine**
Ventral striatum	0.2	0.1	0.4	0.3	0.2	0.5
Dorsal striatum	0.2	0.1	0.3	0.1	0.1	0.2

Table 8. *BP of [^{11}C]RGH-1756 in the ventral and the dorsal striatum in three monkeys measured in baseline examinations and after administration of reserpine. BP was calculated as the ratio of specific to non-specific binding after the integration of the TACs between 9-45 minutes of the examination as described in 'Experimental procedures'.*

4.3. INCREASING THE ACCURACY OF *IN VIVO* QUANTIFICATION OF DOPAMINE-D_2/D_3 RECEPTORS IN THE HUMAN BRAIN BY PARTIAL VOLUME EFFECT CORRECTION (PAPERS IV AND V)

Despite of the well-known influence of PVE on quantitative PET measurements, systematic investigation of the effect of PVE on the most commonly used receptor binding parameters, such as BP, DV_{tot} and kinetic rate constants, has not yet been performed. A few studies examined the influence of PVE on observed [^{18}F]DOPA (Rousset et al. 2000) and [^{11}C]raclopride (Yokoi et al. 1998) binding. The first study demonstrated that apparent net blood-brain clearance and the equilibrium distribution volume of [^{18}F]DOPA, and the relative activity of dopa decarboxylase were significantly underestimated in the human striatum due to PVEs (Rousset et al. 2000). The latter study showed that BP (k_3/k_4) of [^{11}C]raclopride is underestimated without PVE correction by 71% and 44% in caudate and putamen, respectively (Yokoi et al. 1998).

The PET studies reported in the following sections had a two-fold aim: (i) to estimate the influence of PVE on quantitative PET studies with [^{11}C]FLB 457 and [^{11}C]raclopride in the human brain and (ii) to evaluate the relevance of a ROI based PVE correction method (Rousset et al. 1998a) with the purpose to formulate recommendations on the application of PVE correction in PET studies with these two D_2/D_3 selective radioligands.

The standard 2-TCM with simulated arterial input function was used to calculate kinetic rate constants (K_1-k_4), BP and DV_{tot} of [^{11}C]FLB 457 and [^{11}C]raclopride before and after PVE correction, as described in detail above.

4.3.1. Volumetry and calculation of recovery coefficient

PVE correction, according to Roussset et al. (1998a), relies on geometric and volumetric information obtained from high-resolution MR images. To perform PVE correction a number of regions were segmented manually and their volumes were measured (Table 9). Results of the volumetric measurements were generally in good agreement with previously published data, considering that the subjects examined in the present study were older than in previous ones (for comparison see the following refs. on striatum (Gunning-Dixon et al. 1998; Krishnan et al. 1990; Raz et al. 2003), thalamus (Gilbert et al. 2001), insula (Crespo-Facorro et al. 2000; Kasai et al. 2003), anterior cingulate (Ballmaier et al. 2004), hippocampus and amygdala (Bonilha et al. 2004; Niemann et al. 2000; Pruessner et al. 2000).

The RC of each region was derived from the matrix of transfer coefficients used for PVE correction. The variability of RC between different brain regions was small (0.42-0.66). The lowest RC value was calculated in the smallest and the thinnest structures, ventral striatum and anterior cingulate. The highest values were obtained in the largest structures, WM and cerebellum. The inter-individual variability of regional RC values was small (Table 9). Despite of the small differences in regional RC between subjects a highly significant correlation was found between the volumes of the structure and the corresponding RC value for all striatal and thalamic subregions and hippocampus.

The low average regional RC values suggest that uptake of [^{11}C]FLB 457 and [^{11}C]raclopride could be severely underestimated throughout the entire brain. The difference of RC between brain regions was small, considering the substantial difference in shape and size of the regions. For some regions, such as caudate, putamen, hippocampus and thalamic subregions, the low RC could largely be explained by the small size of the regions. For neocortical regions the thinness of these structures renders them prone to PVE. The highly significant correlation found between the volume and the RC of some brain regions confirms the results of studies with geometric phantoms performed early during the history of PET imaging (Hoffman et al. 1979; Kessler et al. 1984). These studies demonstrated that the

relationship between the size of a simple geometrical object (cylinder, sphere) and its RC can be described by a sigmoid curve. For objects of a size 0.5-2 times the FHWM of the PET system the relationship between the volume and the RC of the object is linear. No such relationship was found for cortical regions, probably due to the complicated shape and the arising multiple self-interactions within these regions.

	Volume (ml)	**RC**
Ventral striatum	1.2 ± 0.2	0.42 ± 0.02
Dorsal caudate	3.1 ± 0.6	0.50 ± 0.02
Dorsal putamen	4.0 ± 0.4	0.59 ± 0.02
Thalamus	6.4 ± 0.8	-
Lateral thalamus	2.7 ± 0.6	0.59 ± 0.03
Medial thalamus	2.3 ± 0.3	0.53 ± 0.03
Posterior thalamus	1.4 ± 0.3	0.45 ± 0.03
Hippocampal complex	2.8 ± 0.4	0.45 ± 0.03
Insular cortex	5.8 ± 0.6	0.45 ± 0.03
Anterior cingulate	7.6 ± 1.7	0.42 ± 0.03
Temporal cortex	84.8 ± 10.6	0.52 ± 0.02
Frontal cortex	90.7 ± 13.3	0.48 ± 0.02
Parietal cortex	50.4 ± 6.2	0.46 ± 0.02
Occipital cortex	30.1 ± 5.1	0.46 ± 0.03
Cerebellum	142.8 ± 17.7	0.63 ± 0.02
White matter	475.5 ± 58.8	0.66 ± 0.01
CSF	559.6 ± 71.8	1.00
Whole brain	1215.3 ± 115.4	-
Intracranial volume	1774.9 ± 132.6	-

Table 9. *Average volume of brain regions (mean ± SD), and the average recovery coefficient (RC). Volume of ventral striatum, dorsal part of caudate and that of putamen was measured in eight subjects, all other volumes were measured in nine subjects. For bilateral structures the measurements were performed on both sides and the results were averaged for each subject.*

4.3.2. Time activity curves for [^{11}C]FLB 457 and [^{11}C]raclopride

The effect of PVE correction on TACs for [^{11}C]FLB 457 and [^{11}C]raclopride binding varied between the regions examined. With the exception of WM all PVE corrected TACs were higher than the corresponding observed ones. The increase of TACs for GM regions after PVE correction varied between 5-70% of the observed values for [^{11}C]FLB 457 and between 40-60% of the observed values for [^{11}C]raclopride. The effect of PVE correction on regional TACs varied with time for both radioligands, thus not only the amplitude but also the shape of regional TACs was changed after PVE correction. Analysis of the transfer coefficient matrices revealed that changes of the TACs after PVE correction can partly be explained by the varying degree of self-interaction (regional RC values), and partly by the

spill-in of activity from neighbouring regions. Former factor (RC) was responsible for the changes of the amplitude of the TACs, whereas spill-in was important for the alterations in the shape of the curves.

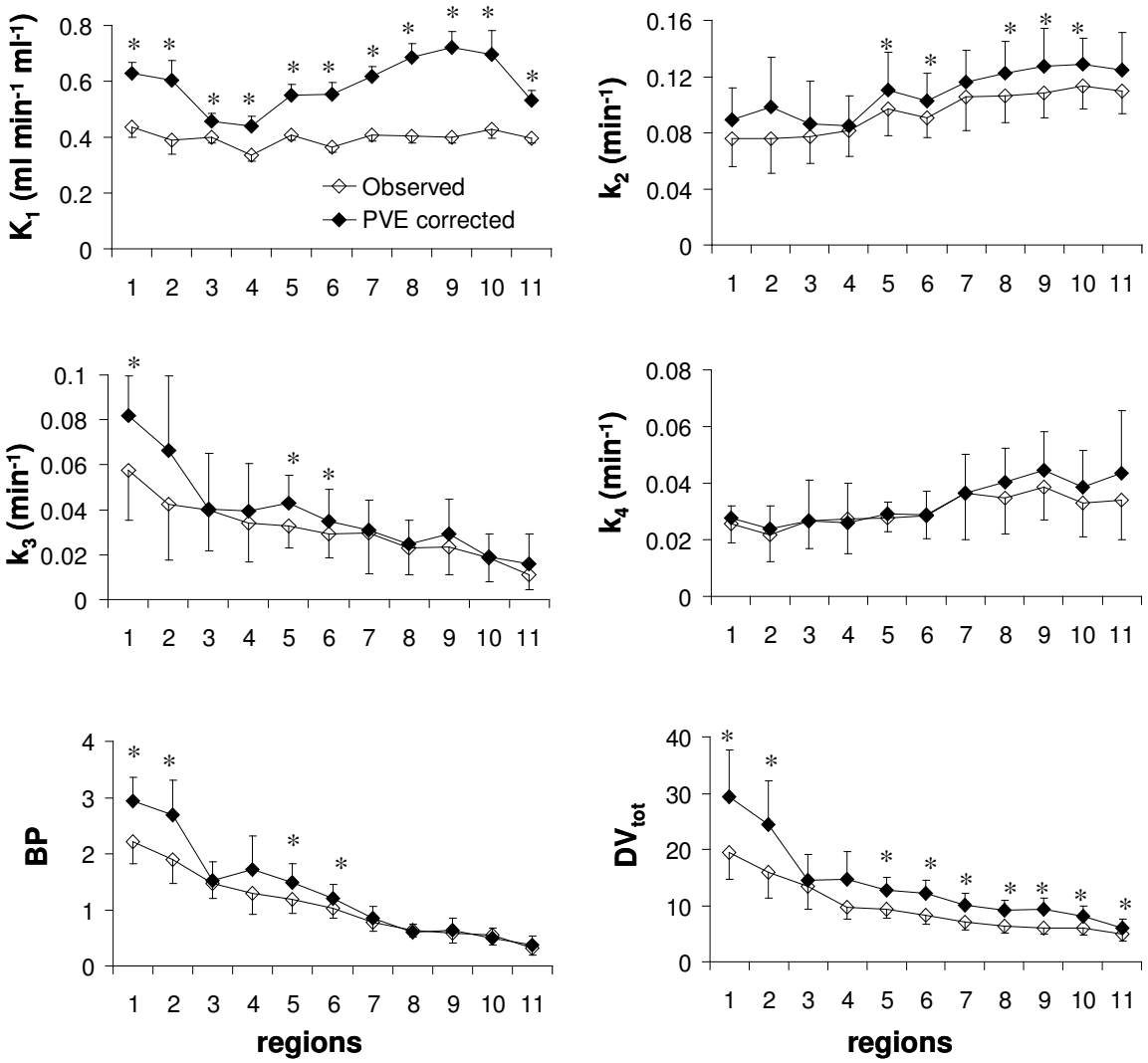

Figure 13. *Rate constants, BP and DV_{tot} of [^{11}C]FLB 457 before and after PVE correction. Observed values are denoted by empty signs (mean-SD), whereas PVE corrected values are represented by filled signes (mean+SD). The brain regions examined are: 1. med. thalamus, 2. post. thalamus, 3. lat. thalamus, 4. hippocampal complex, 5. insular cortex, 6. temporal cortex, 7. ant. cingulate, 8. frontal cortex, 9. parietal cortex, 10. occipital cortex, 11. cerebellum. *, Significant difference between observed and PVE corrected values, ($p<0.05$, Bonferroni corrected).*

4.3.3. Kinetic rate constants

Observed and PVE corrected TACs for [^{11}C]FLB 457 and [^{11}C]raclopride were entered into kinetic analysis of radioligand binding to calculate the rate constants. PVE correction had different effect on rate constants of [^{11}C]FLB 457 and [^{11}C]raclopride. The

results demonstrated that rate constants of [^{11}C]FLB 457 are more susceptible to PVE than those of [^{11}C]raclopride.

PVE correction had a significant overall effect on all four rate constants (K_1-k_4) of [^{11}C]FLB 457 (Figure 13). Planned comparisons were used to identify the regions, where the individual k values were changed after PVE correction. For [^{11}C]FLB 457 PVE correction had the largest effect on K_1, as this rate constant was increased in all regions examined. k_2 was increased in most cortical regions, k_3 was increased in temporal and insular cortices and medial thalamus, whereas k_4 was hardly changed after PVE correction. SD of all rate constants was increased after PVE correction for both radioligands.

PVE correction induced a significant increase in K_1 and k_3 of [^{11}C]raclopride, whereas k_2 and k_4 were not changed (Figure 14). K_1 was significantly increased in the dorsal caudate and putamen but not in the ventral striatum, whereas k_3 was increased in the entire striatum.

Changes of amplitude and shape of the TACs translated into changes of the rate constants of [^{11}C]FLB 457 and [^{11}C]raclopride. K_1 was significantly increased in almost all regions after PVE correction, indicating that the transport rate of [^{11}C]FLB 457 and [^{11}C]raclopride from plasma to brain is significantly underestimated throughout the whole brain. The simulataneous increase of K_1 and k_2 in cortical regions indicates that the rate of ligand exchange between plasma and tissue is significantly underestimated without PVE correction. k_3 was increased after PVE correction in brain regions, which are known to contain moderate to high densities of D_2/D_3 receptors. As k_3 is the most closely related to B_{max} it can be assumed that the density of D_2/D_3 receptors would be underestimated in these regions if PVE correction was not applied.

4.3.4. Binding potential

Binding potential was calculated as k_3/k_4 for both radioligands. The effect of PVE correction on BP of [^{11}C]FLB 457 varied between regions to a great extent. Statistical analysis revealed that PVE correction induced a significant increase in BP in temporal and insular cortices, medial and posterior thalamus. The rank order of regional BP values was slightly changed after PVE correction.

PVE correction had a significant effect on BP of [^{11}C]raclopride in all subregions of the striatum. BP was increased by 30-50% after PVE correction, and the highest increase was observed in the ventral striatum. SD of BP was substantially increased in all regions after PVE correction for [^{11}C]FLB 457 and [^{11}C]raclopride.

Changes in BP of [^{11}C]FLB 457 and [^{11}C]raclopride after PVE correction were in accordance with changes of the rate constants. Increase of BP also indicated that density of D_2/D_3 receptors was underestimated without PVE correction in a few brain regions. No correlation was found between the volume of brain regions and the increase of BP after PVE correction. It is therefore not possible to predict in advance the exact degree of underestimation of BP due to PVE, the correction has to be performed for each individual.

4.3.5. Total volume of distribution

The total volume of distribution (DV_{tot}) was calculated as a complex of rate constants, as defined above. PVE correction had a substantial influence on DV_{tot} of [^{11}C]FLB 457 and [^{11}C]raclopride.

For [^{11}C]FLB 457 the smallest increase of DV_{tot} was observed in the lateral thalamus (8%), whereas the highest increase was measured in the posterior thalamus and the parietal cortex (54% and 57%, respectively). SD of DV_{tot} was also increased after PVE correction for [^{11}C]FLB 457. No correlation was found between regional volumes and rate of increase of DV_{tot} after PVE correction in any extrastriatal brain areas.

DV_{tot} of [^{11}C]raclopride was significantly increased in all subregions of the striatum after PVE correction. The relationship between volume of brain structures and PVE correction induced increase of DV_{tot} was examined by linear regression. In the ventral striatum no correlation was found between the two parameters. In the dorsal part of putamen and that of caudate, however, there was a tendency towards significant negative correlation between volume of the structures and the change of DV_{tot} after PVE correction.

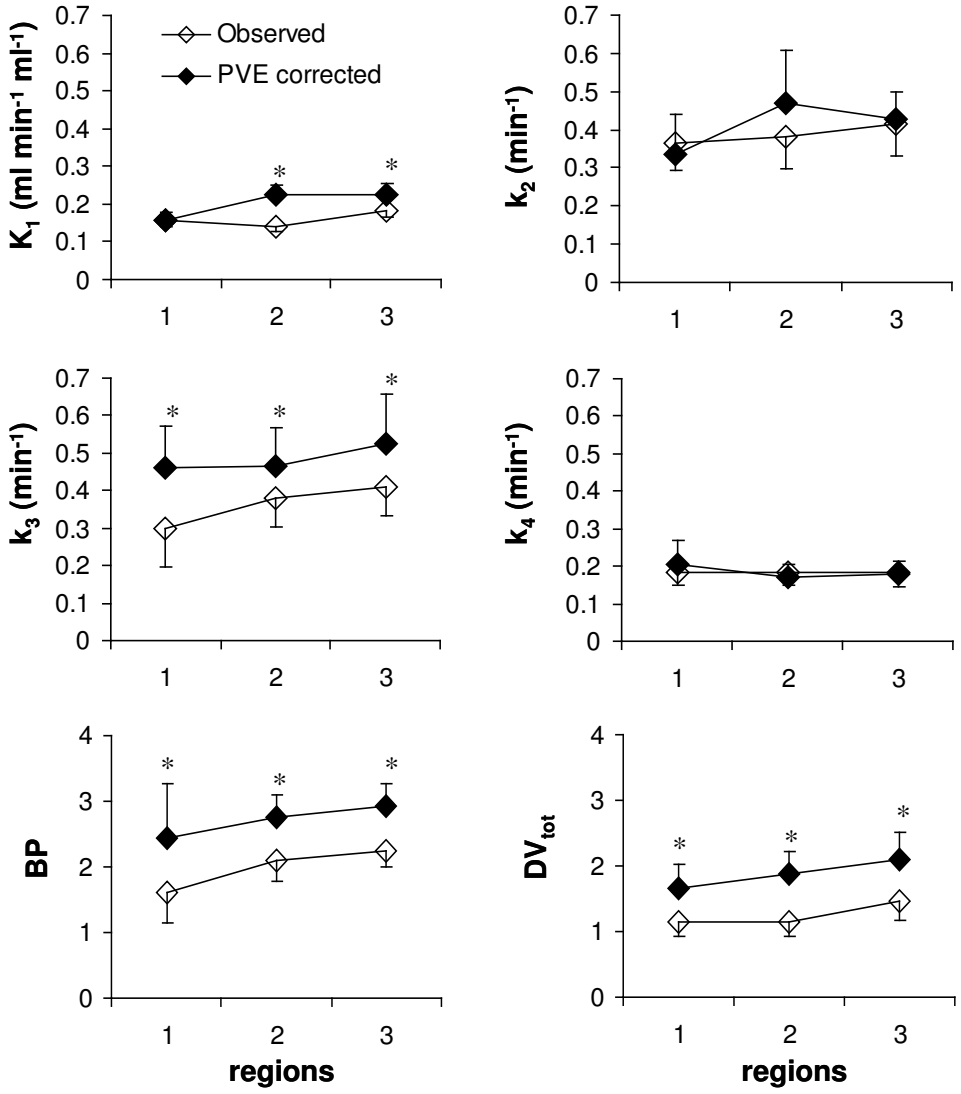

Figure 14. *Rate constants, BP and DV_{tot} of [^{11}C]raclopride before and after PVE correction. Observed values are denoted by empty signs (mean-SD), whereas PVE corrected values are represented by filled signes (mean+SD). The brain regions examined are: 1. ventral striatum, 2. dorsal caudate, 3. dorsal putamen. *, Significant difference between observed and PVE corrected values, ($p<0.05$, Bonferroni corrected).*

Increase of BP after PVE correction partly explains the increase of total distribution volume of [^{11}C]FLB 457 and [^{11}C]raclopride. For most regions, higher K_1 values also contributed to the measured substantial increase of DV_{tot}. An explanation to the large increase of DV_{tot} after PVE correction could be deduced from the pharmacological interpretation of the parameter, which states that DV_{tot} is equal to the ratio of the radioligand concentration in

tissue to plasma at equilibrium. As radioactivity concentration is compromised by PVE in tissue, but not in plasma, their ratio would be underestimated without correcting tissue radioactivity concentration for PVE. The degree to which tissue radioactivity concentration is compromised by PVE depends largely on the regional RC, which is, in turn, determined by the volume of the region, provided that the shape of the region is rather simple. This explains the tendency for significant negative correlation between volume of a regions and the rate of increase in DV_{tot} for striatal subregions.

4.3.6. Application of PVE correction in clinical PET studies

Results of the present study demonstrated that PVE has sizeable effect on the observed TACs and binding parameters of [^{11}C]FLB 457 and [^{11}C]raclopride. Therefore the application of PVE correction is highly recommended in all PET studies when volumetric differences are present between the subjects or the groups compared, i.e. for the examination of D_2/D_3 receptors in neurodegenerative disorders or during aging. In such PET studies, PVE correction can compensate for the decrease in observed radioactivity concentration caused by regional brain atrophy in comparisons with healthy subjects.

Application of PVE correction could also be useful in studies where the true values of receptor-binding parameters are of interest, for example in calculation of receptor density (B_{max}) and ligand affinity (K_d) in Scatchard analysis.

In routine clinical studies with [^{11}C]FLB 457 and [^{11}C]raclopride, where no between-group differences are detected in the volume of the brain regions, PVE correction is not essential since the same degree of underestimation of the binding parameters can be expected in both groups. Nevertheless, PVE correction could be useful for the detection of small changes in radioligand binding by improving the contrast between different regions of the brain. Previous studies (Kessler et al. 1984) have demonstrated that the true increase in radioactivity concentration is higher than the observed increase, and thereby small changes in radioactivity concentration might be undetectable without PVE correction. PVE correction can therefore help to detect small changes in radioligand binding in patients compared to control subjects, which would otherwise be overlooked. In the present study only healthy comparison subjects were examined; and thus, further studies are needed to clarify this question.

Some aspects of PVE correction, however, might limit its application in clinical PET studies. One such aspect is the inherent depreciation of precision. The higher SD of receptor binding parameters after PVE correction could hinder the detection of between group differences. The other limitation of PVE correction is that its results are influenced by segmentation errors. Such errors propagate through the entire process of analysis and can finally lead to incorrect estimates for receptor binding parameters. This phenomenon can be observed in the present study for hippocampus, ventral striatum and cerebellum. PVE corrected K_1 of hippocampus and ventral striatum is lower than K_1 in other regions, probably because of segmentation errors, i.e. WM was included in the ROI of these structures. It was not possible to completely separate GM and WM in the cerebellar hemispheres. Therefore, cerebellum was considered as a large GM region by the correction algorithm, which resulted in incomplete PVE correction. PVE corrected TAC of the cerebellum does not give a reliable estimate of nonspecific binding, which prohibits the application of reference tissue methods for the calculation of BP for [^{11}C]FLB 457 and [^{11}C]raclopride. Arterial input function is necessary for the calculation of receptor binding parameters after PVE correction, which might not always be accomplishable in clinical PET studies. Thus, in clinical studies the benefits of PVE correction (higher accuracy of parameters and improved contrast between brain regions) and its drawbacks (loss of precision and necessity of arterial blood sampling) must be considered at the same time.

5. SUMMARY AND FUTURE PROSPECTS

The present thesis focused on examining three thus far unexplored aspects of dopamine-D_2/D_3 receptors by the application of newly established techniques.

In Paper I, the first application of agonist stimulated [^{35}S]GTPγS binding autoradiography is reported for studies on D_2/D_3 receptors in the human brain. The present study has shown that this technique is suitable for the examination of dopamine-D_2/D_3 receptors in the *postmortem* human brain. The functional response to DA, the physiological agonist, and to qunpirole, a prototype D_2/D_3 agonist, was described in human whole hemisphere cryosections. The results indicated that this method could be a suitable tool for the examination of coupling between D_2/D_3 receptors and G proteins in neuropsychiatric diseases. Alterations of the interaction between D_2/D_3 receptors and G proteins were suggested in disorders such as schizophrenia or Parkinson disease. DA stimulated [^{35}S]GTPγS binding autoradiography could thus be a potential method to examine the function of D_2/D_3 receptors and G proteins in these conditions.

A drawback of agonist stimulated [^{35}S]GTPγS binding autoradiography is that it is limited to the examination of receptors coupled to pertussis toxin-sensitive G proteins (Happe et al. 2001; Sim et al. 1995). The inability to detect receptor stimulation through G_s is probably due to the slower dissociation of GDP from G_s compared to G_o and G_i (Carty & Iyengar, 1994; Weiland & Jakobs, 1994). Therefore D_1 and D_5 receptors cannot be studied today using this technique. For the functional examination of D_1/D_5 receptors, the development of new techniques is necessary or, if possible, the modification of the present assay is needed.

It is becoming increasingly evident that molecules involved in signal transduction are not randomly scattered in the cell membrane and within the cytosol, but are organised in functional compartments of the cell, termed caveolae. Plasmalemmal caveolae are specialized microdomains in the cell, enriched in a large number of signaling molecules, including GPCR, and G proteins and their effectors, such as protein-kinases, adenylyl cyclase and molecules involved in Ca^{2+} dependent signaling (reviewed in Shaul & Anderson, 1998). Caveolae are rather stable structures, for example they are resistant to solubilisation by Triton X-100. This raises the possibility that signalling pathways of GPCR could be studied by autoradiographic methods even beyond the interaction with G proteins. Naturally, examination of further steps of the signalling pathway involves a number of difficulties, such as synthesis of suitable radioligands and the establishment of the appropriate assay conditions. The radioligands, such as [^{35}S]GTPγS, should be analogues of the endogenous substrates but must be resistant to metabolism. Establishment of the appropriate assay conditions might be difficult, since *in vitro* interaction of several molecules would be necessary for the activation of effectors. It is questionable whether all these molecules can be preserved in tissue sections in such a state that ensures possible interaction with other signalling molecules. On the other hand, establishment of an assay capable of examining the activation of second messenger systems and effectors *in situ* in tissue sections, could clarify many so far unknown aspects of intracellular signalling of GPCRs.

Paper II and III report an attempt on the selective *in vivo* labelling of dopamine-D_3 receptors in the brain with PET. The binding characteristics of the putative D_3-selective radioligand, [^{11}C]RGH-1756 were described in the monkey brain. Previous *in vitro* radioligand binding studies have demonstrated high-affinity and high selectivity of RGH-1756 binding to D_3 receptors (Kiss et al. 2000; Laszlovszky et al. 2000). Despite the promising *in vitro* characteristics of the molecule, [^{11}C]RGH-1756 yielded very low signal for specific D_3 binding in the monkey brain. Pretreatment with unlabelled RGH-1756 inhibited

binding of the radioligand, suggesting saturable binding of [^{11}C]RGH-1756. After administration of raclopride, the binding of [^{11}C]RGH-1756 was slightly lower, which could indicate that [^{11}C]RGH-1756 binds to D_2/D_3 receptors in the monkey brain. The signal for specific binding of [^{11}C]RGH-1756 was, however, so small that observed effects of the pretreatment drugs could be confounded by noise of the measurements. The low specific binding of [^{11}C]RGH-1756 was somewhat unexpected, as RGH-1756 showed favourable binding characteristcs in previous *in vitro* experiments. It has been suggested that D_3 receptors are occupied by endogenous DA to a high degree (Levant, 1995; Schotte et al. 1992, 1996). As DA has very high affinity for the D_3 receptor (Sokoloff et al. 1990), it is possible that the endogenous transmitter could prevent the binding of [^{11}C]RGH-1756 to D_3 receptors. To test this hypothesis the effect of reserpine induced DA depletion was examined on the binding of [^{11}C]RGH-1756 in the monkey brain. After reserpine treatment there was no consistent increase in specific binding of [^{11}C]RGH-1756. This observation does not support the assumption that binding of [^{11}C]RGH-1756 to D_3 receptors is inhibited by high occupancy of D_3 receptors by endogenous DA. The possible reason for low specific binding of [^{11}C]RGH-1756 is, therefore, the low *in vivo* affinity of the compound. Despite the promising *in vitro* results, [^{11}C]RGH-1756 is not suitable for *in vivo* examination of D_3 receptors. The results of the studies with [^{11}C]RGH-1756 point of that labelling of receptors with such low densities as the D_3 receptors requires ligands with very high affinity and selectivity.

Several radioligands have previously been considered for *in vitro* imaging of the D_3 receptor. [^{3}H]7-OH-DPAT and [^{3}H]PD 128907, two partial agonists, have been most extensively used in studies on the D_3 receptor. 7-OH-DPAT has about 78 times higher affinity for D_3 than for D_2 receptors (Table 3, Levesque et al. 1992). PD 128907 is somewhat less selective, as it has about 14 times higher affinity for D_3 than for D_2 receptors (Pugsley et al. 1995). The selectivity of pramipexole, another D_3 preferring agonist used in patients with Parkinson disease, is similar to that of PD 128907 (Camacho-Ochoa et al. 1995). None of these D_3 preferring compounds has been used as a radioligand in *in vivo* imaging studies. However, their affinity and selectivity profiles in comparison to that of RGH-1756 suggest that they are probably not ideal for *in vivo* imaging of the D_3 receptor. Therefore, the development of novel compounds is probably necessary for selective *in vivo* labelling of D_3 receptors.

In papers IV and V, the influence of PVE was estimated on the quantification of [^{11}C]FLB 457 and [^{11}C]raclopride binding in the human brain. Changes of the kinetic rate constants, BP and DV_{tot} of the two radioligands, as derived from the standard 2-TCM, were evaluated in the brain after PVE correction. PVE correction altered the amplitude and the shape of TACs of [^{11}C]FLB 457 and [^{11}C]raclopride in most brain regions, which was reflected in the kinetic rate constants and the derived receptor binding parmeters. The effect of PVE correction was different for the two D_2/D_3 specific radioligands due to the different levels of radioligand uptake in distinct regions of the brain. Observed binding of [^{11}C]FLB 457 was extremely high in the striatum and moderate or low, yet measurable in extrastriatal regions. The effect of PVE correction on parameters of [^{11}C]FLB 457 binding varied to a large extent between the extrastriatal regions examined, depending on the size, shape and the D_2/D_3 receptor density of the regions. [^{11}C]raclopride uptake reached high level in the striatum, but radioligand concentration was very low in all other brain areas. The influence of PVE correction on binding parameters of [^{11}C]raclopride was similar for the three examined subdivisions of the striatum.

PVE had a sizeable effect on the observed uptake of [^{11}C]FLB 457 and that of [^{11}C]raclopride in the human brain. A significant correlation was found between the regional volume and recovery coefficient in some brain regions, indicating that volume of the regions

could be an important factor for the degree of underestimation of observed radioactivity concentration as compared to the true values. However, spill-in of radioactivity from surrounding tissue compartments also contributed to the observed regional radioactivity concentration. This implies that knowing the volume of a region within the brain is insufficient to draw conclusions about the resulting PVEs. Interactions between the different regions have to be considered, as well. In line with the previous statement, no significant correlation was found between regional volume and regional increase of either BP or DV_{tot} after PVE correction. Although a tendency was observed towards a negative correlation between regional volume and increase of DV_{tot} for [^{11}C]raclopride after PVE correction in the dorsal putamen. Volume of brain regions, however, is a poor predictor of changes in binding parameters after PVE correction. It is therefore not possible to predict the effect of PVE on regional binding parameters, and PVE correction has to be performed in each individual case.

In the present work some recommendations were also made on the application of PVE correction in clinical PET studies. Both the advantages and drawbacks of PVE correction have to be considered when PVE correction is applied in PET studies. The advantages are increased accuracy of measurements and improved inter-regional contrast of radioligand uptake within the brain. The disadvantages are the loss of precision of the measurements and the susceptibility of the PVE correction algorithm to segmentation errors.

For the future, the development of such PVE correction algorithms would be beneficial, which are free from drawbacks of the presently used method. Amplification of noise is a huge problem of the currently used PVE correction method, as it can hinder quantification of radioligand uptake in small regions. Some errors in PVE corrected TACs of [^{11}C]raclopride and [^{11}C]FLB 457 were also observed using the present algorithm, most likely due to inaccurate segmentation of gray and white matter. To solve this problem the development of a new method would be necessary, which could handle tissue fraction effects better than the present method.

6. ACKNOWLEDGEMENTS

It has been a long and bumpy road, but I had the privilege and the pleasure of being accompanied by many people. I want to express my most sincere gratitude to everyone, who contributed to this thesis with his or her knowledge, talent, and enthusiasm and who have been supportive during all these years.

Assoc. Prof. Balázs Gulyás, my main tutor, for the possibility to study at KI, inviting me to the PET group, for his support, enthusiasm, and teaching me to always look for the basic principles behind the complicatedness of brain function, to set details into a broader frame and to never stop wondering about the potentials of the human brain.

Prof. Lars Farde, my co-tutor, for highly valuable, thorough and critical guidance through the world of molecular imaging, finding time for meetings in his extremely tight schedule, inspiring discussions on historical and future perspectives of PET, and teaching me to value the art of scientific writing.

Assoc. Prof. Håkan Hall, my co-tutor, for his support and commitment to our common research project, and for introducing me into the world of neuroreceptors, while sharing with me his great research knowledge on dopamine, and teaching me to appreciate the difficulties and the value of laboratory work.

Participants of the PVEOut project, Drs. Mario Quarantelli, Claus Svarer, Ali Hojjat, Karim Berkouk, Prof. Alan Colchester and Marco Comerci, for patiently answering an endless list of technical questions about PET and PVE, making such good software, and for humour and enthusiasm.

Prof. Christer Halldin for expert knowledge in radiochemistry, enthusiasm and devotedness for developing new PET radioligands and the resulting many co-authorships.

Chief veterinarian Mats Spångberg and the animal care-takers at SMI for cooperativeness, flexibility and for taking such good care of the monkeys.

Kjerstin Lind for warmth and understanding and for encouraging me to speak Swedish, for helping me with various things in the PET group, and for the apple cakes.

Kerstin Larsson for helping me to find my way in the lab, and for keeping the laboratory and its equipment in perfect order.

The radiochemistry group, in particular Oliver Langer, Evgenij Schukin, Magnus Schou, Jari Tarkiainen and Sjoerd Finnema, for radioligand sythesis, for dissolving all insoluble compounds and for patiently tolerating me on my off-days during our numerous common works.

Barbro Berthelsson and Alexandra Tylec for being helpful in the lab.

Nils Sjöholm for the phantom measurements and for much valuable information about the camera.

Katarina Varnäs for sharing with me her knowledge and experience about autoradiography.

My colleges at the PET group: Dr. Hans Olsson for extremely useful discussions about kinetic modelling, Zsolt Cselényi for the excellent converters, Dr. Simon Červenka for precision in our common work, Hristina Jovanovic and Jacqueline Borg for spicing up life on the PET corridor, and for the many pleasant common breaks, Dr Bengt Andrée for cheerfulness and Dr

Mirjam Talvik for many interesting discussions about research and life in general and for help when it was needed so much.

My 'room-mates': Johan Lundberg for discussions on research, philosophy, psychiatry and everything else, and for a great sense of humour, and Nina Erixon for being such a nice person and for showing me one of the most beautiful places in Sweden.

Aurelija Jučaitė for friendship, for sharing with me her thoughts about the world and people in it, for the warm-hearted company in cold Lappland, where she always found the right path. Special thanks for the help with printing this thesis.

Helga and Lasse Ivéus for care and warm welcome, for all the delicious dinners and for making me feel at home in Stockholm.

My sister Krisztina for the many cups of coffee before the early flights to Sweden, and my cousin Edit for the innumerable cheese-cookies.

My Mum and Dad for their complete, and never ending support.

This work was supported by the 5th Framework Programme of the European Community (PVEOut project, contract QLG3-CT2000-00594), Gedeon Richter Ltd., Hungary, Svenska Institutet, the Hungarian Scholarship Committee, the Hungarian State Eötvös Scholarship, the Professor Bror Gadelius Minnesfond.

7. REFERENCES

Alvaro, J., Cummings, J.A., Duman, C., Glatt, C., Van Koughnet, K., Krantz, D., McBain, C., Neylan, T., Rieff, H., Ullrich, N. & Wolf, D. (2001). Catecholamines. In *Molecular Neuropharmacology: A Foundation for Clinical Neuroscience*, Nestler, E.J., Hyman, S.E. & Malenka, R.C. (eds). pp 167-190. The McGraw-Hill Companies, Inc.: New York.

Andreasen, N.C., Rajarethinam, R., Cizadlo, T., Arndt, S., Swayze, V.W., 2nd, Flashman, L.A., O'Leary, D.S., Ehrhardt, J.C. & Yuh, W.T. (1996). Automatic atlas-based volume estimation of human brain regions from MR images. *J Comput Assist Tomogr*, **20,** 98-106.

Ashburner, J. & Friston, K. (1997). Multimodal image coregistration and partitioning–a unified framework. *Neuroimage*, **6,** 209-17.

Aston, J.A., Cunningham, V.J., Asselin, M.C., Hammers, A., Evans, A.C. & Gunn, R.N. (2002). Positron emission tomography partial volume correction: estimation and algorithms. *J Cereb Blood Flow Metab*, **22,** 1019-34.

Bailey, D.L. & Parker, J.A. (2004). Single-photon emission computed tomography. In *Nuclear medicine in clinical diagnosis and treatment*, Ell, P.J. & Gambhir, S.S. (eds) pp. 1815-1826. Churchill Livingstone: Edinburgh, London, New York, Oxford, Philadelphia, San Francisco, Sydney.

Baldwin, J.M. (1993). The probable arrangement of the helices in G protein-coupled receptors. *Embo J*, **12,** 1693-703.

Ballmaier, M., Toga, A.W., Blanton, R.E., Sowell, E.R., Lavretsky, H., Peterson, J., Pham, D. & Kumar, A. (2004). Anterior cingulate, gyrus rectus, and orbitofrontal abnormalities in elderly depressed patients: an MRI-based parcellation of the prefrontal cortex. *Am J Psychiatry*, **161,** 99-108.

Bancroft, G.N., Morgan, K.A., Flietstra, R.J. & Levant, B. (1998). Binding of [^{3}H]PD 128907, a putatively selective ligand for the D_3 dopamine receptor, in rat brain: a receptor binding and quantitative autoradiographic study. *Neuropsychopharmacology*, **18,** 305-16.

Bergstrom, M., Boethius, J., Eriksson, L., Greitz, T., Ribbe, T. & Widen, L. (1981). Head fixation device for reproducible position alignment in transmission CT and positron emission tomography. *J Comput Assist Tomogr*, **5,** 136-41.

Bonilha, L., Kobayashi, E., Cendes, F. & Min Li, L. (2004). Protocol for volumetric segmentation of medial temporal structures using high-resolution 3-D magnetic resonance imaging. *Hum Brain Mapp*, **22,** 145-54.

Buchsbaum, M.S., Someya, T., Teng, C.Y., Abel, L., Chin, S., Najafi, A., Haier, R.J., Wu, J. & Bunney, W.E., Jr. (1996). PET and MRI of the thalamus in never-medicated patients with schizophrenia. *Am J Psychiatry*, **153,** 191-9.

Byne, W., Buchsbaum, M.S., Mattiace, L.A., Hazlett, E.A., Kemether, E., Elhakem, S.L., Purohit, D.P., Haroutunian, V. & Jones, L. (2002). Postmortem assessment of thalamic nuclear volumes in subjects with schizophrenia. *Am J Psychiatry*, **159,** 59-65.

Camacho-Ochoa, M., Walker, E.L., Evans, D.L. & Piercey, M.F. (1995). Rat brain binding sites for pramipexole, a clinically useful D_3-preferring dopamine agonist. *Neurosci Lett*, **196,** 97-100.

Camps, M., Cortes, R., Gueye, B., Probst, A. & Palacios, J.M. (1989). Dopamine receptors in human brain: autoradiographic distribution of D_2 sites. *Neuroscience*, **28,** 275-90.

Camus, A., Javoy-Agid, F., Dubois, A. & Scatton, B. (1986). Autoradiographic localization and quantification of dopamine D_2 receptors in normal human brain with [^{3}H]N-n-propylnorapomorphine. *Brain Res*, **375,** 135-49.

Carlsson, A., Lindqvist, M., Magnusson, T. & Waldeck, B. (1958). On the presence of 3-hydroxytyramine in brain. *Science*, **127,** 471.

Carlsson, M.L., Carlsson, A. & Nilsson, M. (2004). Schizophrenia: from dopamine to glutamate and back. *Curr Med Chem*, **11,** 267-77.

Carty, D.J. & Iyengar, R. (1994). Guanosine 5'-(γ-thio)triphosphate binding assay for solubilized G proteins. *Methods Enzymol*, **237,** 38-44.

Chio, C.L., Lajiness, M.E. & Huff, R.M. (1994). Activation of heterologously expressed D_3 dopamine receptors: comparison with D_2 dopamine receptors. *Mol Pharmacol*, **45,** 51-60.

Chou, Y.H., Karlsson, P., Halldin, C., Olsson, H. & Farde, L. (1999). A PET study of D_1-like dopamine receptor ligand binding during altered endogenous dopamine levels in the primate brain. *Psychopharmacology (Berl)*, **146,** 220-7.

Coldwell, M.C., Boyfield, I., Brown, A.M., Stemp, G. & Middlemiss, D.N. (1999a). Pharmacological characterization of extracellular acidification rate responses in human $D_{2(long)}$, D_3 and $D_{4.4}$ receptors expressed in Chinese hamster ovary cells. *Br J Pharmacol*, **127,** 1135-44.

Coldwell, M.C., Boyfield, I., Brown, T., Hagan, J.J. & Middlemiss, D.N. (1999b). Comparison of the functional potencies of ropinirole and other dopamine receptor agonists at human $D_{2(long)}$, D_3 and $D_{4.4}$ receptors expressed in Chinese hamster ovary cells. *Br J Pharmacol*, **127,** 1696-702.

Cragg, S.J., Hille, C.J. & Greenfield, S.A. (2000). Dopamine release and uptake dynamics within nonhuman primate striatum in vitro. *J Neurosci*, **20,** 8209-17.

Cragg, S.J., Hille, C.J. & Greenfield, S.A. (2002). Functional domains in dorsal striatum of the nonhuman primate are defined by the dynamic behavior of dopamine. *J Neurosci*, **22,** 5705-12.

Crespo-Facorro, B., Kim, J., Andreasen, N.C., O'Leary, D.S., Bockholt, H.J. & Magnotta, V. (2000). Insular cortex abnormalities in schizophrenia: a structural magnetic resonance imaging study of first-episode patients. *Schizophr Res*, **46,** 35-43.

Culm, K.E., Lim, A.M., Onton, J.A. & Hammer, R.P., Jr. (2003). Reduced G_i and G_o protein function in the rat nucleus accumbens attenuates sensorimotor gating deficits. *Brain Res*, **982,** 12-8.

Cumming, P., Wong, D.F., Gillings, N., Hilton, J., Scheffel, U. & Gjedde, A. (2002). Specific binding of [^{11}C]raclopride and N-[^{3}H]propyl-norapomorphine to dopamine receptors in living mouse striatum: occupancy by endogenous dopamine and guanosine triphosphate-free G protein. *J Cereb Blood Flow Metab*, **22,** 596-604.

De Keyser, J., Claeys, A., De Backer, J.P., Ebinger, G., Roels, F. & Vauquelin, G. (1988). Autoradiographic localization of D_1 and D_2 dopamine receptors in the human brain. *Neurosci Lett*, **91,** 142-7.

De Lean, A., Stadel, J.M. & Lefkowitz, R.J. (1980). A ternary complex model explains the agonist-specific binding properties of the adenylate cyclase-coupled β-adrenergic receptor. *J Biol Chem*, **255,** 7108-17.

Diaz, J., Levesque, D., Lammers, C.H., Griffon, N., Martres, M.P., Schwartz, J.C. & Sokoloff, P. (1995). Phenotypical characterization of neurons expressing the dopamine D_3 receptor in the rat brain. *Neuroscience*, **65,** 731-45.

Eberl, S. & Zimmermann, R.E. (2004). Nuclear medicine imaging instrumentation. In *Nuclear medicine in clinical diagnosis and treatment*, Ell, P.J. & Gambhir, S.S. (eds) pp. 1765-1775. Churchill Livingstone: Edinburgh, London, New York, Oxford, Philadelphia, San Francisco, Sydney.

Elsworth, J.D. & Roth, R.H. (1997). Dopamine synthesis, uptake, metabolism, and receptors: relevance to gene therapy of Parkinson's disease. *Exp Neurol*, **144,** 4-9.

Endres, C.J., Kolachana, B.S., Saunders, R.C., Su, T., Weinberger, D., Breier, A., Eckelman, W.C. & Carson, R.E. (1997). Kinetic modeling of [^{11}C]raclopride: combined PET-microdialysis studies. *J Cereb Blood Flow Metab*, **17,** 932-42.

Eriksson, L., Dahlblom, M. & Widen, L. (1989). Positron emission tomography - a new for studies of the central nervous system. *J Microscopy*, **157,** 305-333.

Farde, L., Eriksson, L., Blomquist, G. & Halldin, C. (1989). Kinetic analysis of central [^{11}C]raclopride binding to D_2-dopamine receptors studied by PET−a comparison to the equilibrium analysis. *J Cereb Blood Flow Metab*, **9,** 696-708.

Farde, L., Ginovart, N., Ito, H., Lundkvist, C., Pike, V.W., McCarron, J.A. & Halldin, C. (1997). PET-characterization of [carbonyl-^{11}C]WAY-100635 binding to 5-HT_{1A} receptors in the primate brain. *Psychopharmacology (Berl)*, **133,** 196-202.

Farde, L., Hall, H., Ehrin, E. & Sedvall, G. (1986). Quantitative analysis of D2 dopamine receptor binding in the living human brain by PET. *Science*, **231,** 258-61.

Farde, L., Wiesel, F.A., Stone-Elander, S., Halldin, C., Nordstrom, A.L., Hall, H. & Sedvall, G. (1990). D_2 dopamine receptors in neuroleptic-naive schizophrenic patients. A positron emission tomography study with [^{11}C]raclopride. *Arch Gen Psychiatry*, **47,** 213-9.

Febo, M., Gonzalez-Rodriguez, L.A., Capo-Ramos, D.E., Gonzalez-Segarra, N.Y. & Segarra, A.C. (2003). Estrogen-dependent alterations in D_2/D_3-induced G protein activation in cocaine-sensitized female rats. *J Neurochem*, **86,** 405-12.

Gether, U. (2000). Uncovering molecular mechanisms involved in activation of G protein-coupled receptors. *Endocr Rev*, **21,** 90-113.

Geurts, M., Hermans, E., Cumps, J. & Maloteaux, J.M. (1999). Dopamine receptor-modulated [^{35}S]GTPγS binding in striatum of 6-hydroxydopamine-lesioned rats. *Brain Res*, **841,** 135-42.

Gilbert, A.R., Rosenberg, D.R., Harenski, K., Spencer, S., Sweeney, J.A. & Keshavan, M.S. (2001). Thalamic volumes in patients with first-episode schizophrenia. *Am J Psychiatry*, **158,** 618-24.

Ginovart, N., Farde, L., Halldin, C. & Swahn, C.G. (1997). Effect of reserpine-induced depletion of synaptic dopamine on [^{11}C]raclopride binding to D_2-dopamine receptors in the monkey brain. *Synapse*, **25,** 321-5.

Griffon, N., Pilon, C., Sautel, F., Schwartz, J.C. & Sokoloff, P. (1997). Two intracellular signaling pathways for the dopamine D_3 receptor: opposite and synergistic interactions with cyclic AMP. *J Neurochem*, **68,** 1-9.

Grigoriadis, D. & Seeman, P. (1985). Complete conversion of brain D_2 dopamine receptors from the high- to the low-affinity state for dopamine agonists, using sodium ions and guanine nucleotide. *J Neurochem*, **44,** 1925-35.

Gunning-Dixon, F.M., Head, D., McQuain, J., Acker, J.D. & Raz, N. (1998). Differential aging of the human striatum: a prospective MR imaging study. *AJNR Am J Neuroradiol*, **19,** 1501-7.

Guo, N., Hwang, D.R., Lo, E.S., Huang, Y.Y., Laruelle, M. & Abi-Dargham, A. (2003). Dopamine depletion and in vivo binding of PET D_1 receptor radioligands: implications for imaging studies in schizophrenia. *Neuropsychopharmacology*, **28,** 1703-11.

Gurevich, E.V. & Joyce, J.N. (1999). Distribution of dopamine D_3 receptor expressing neurons in the human forebrain: comparison with D_2 receptor expressing neurons. *Neuropsychopharmacology*, **20,** 60-80.

Hall, D.A. & Strange, P.G. (1997). Evidence that antipsychotic drugs are inverse agonists at D_2 dopamine receptors. *Br J Pharmacol*, **121,** 731-6.

Hall, H. (1994). Dopamine Receptors: Radioligands for Pharmacological and Biochemical Characterization. In *Dopamine Receptors and Transporters: Pharmacology, Structure and Function*, Nyznik, H.B. (ed) pp. 3-35. Marcel Dekker, Inc.: New York, Basel, Hong Kong.

Hall, H., Farde, L., Halldin, C., Hurd, Y.L., Pauli, S. & Sedvall, G. (1996a). Autoradiographic localization of extrastriatal D_2-dopamine receptors in the human brain using [^{125}I]epidepride. *Synapse*, **23,** 115-23.

Hall, H., Farde, L. & Sedvall, G. (1988). Human dopamine receptor subtypes–in vitro binding analysis using ^{3}H-SCH 23390 and ^{3}H-raclopride. *J Neural Transm*, **73,** 7-21.

Hall, H., Halldin, C., Dijkstra, D., Wikstrom, H., Wise, L.D., Pugsley, T.A., Sokoloff, P., Pauli, S., Farde, L. & Sedvall, G. (1996b). Autoradiographic localisation of D_3-dopamine receptors in the human brain using the selective D_3-dopamine receptor agonist (+)-[^{3}H]PD 128907. *Psychopharmacology (Berl)*, **128,** 240-7.

Hall, H., Halldin, C., Farde, L. & Sedvall, G. (1998). Whole hemisphere autoradiography of the postmortem human brain. *Nucl Med Biol*, **25,** 715-9.

Hall, H., Hurd, Y.L., Pauli, S., Halldin, C. & Sedvall, G. (2001). Human brain imaging post-mortem – whole hemisphere technologies. *Int Rev Psychiatry*, **13,** 12-17.

Hall, H., Sedvall, G., Magnusson, O., Kopp, J., Halldin, C. & Farde, L. (1994). Distribution of D_1- and D_2-dopamine receptors, and dopamine and its metabolites in the human brain. *Neuropsychopharmacology*, **11,** 245-56.

Halldin, C., Farde, L., Hogberg, T., Hall, H., Strom, P., Ohlberger, A. & Solin, O. (1991). A comparative PET-study of five carbon-11 or fluorine-18 labelled salicylamides. Preparation and in vitro dopamine D-2 receptor binding. *Int J Rad Appl Instrum B*, **18,** 871-81.

Halldin, C., Farde, L., Hogberg, T., Mohell, N., Hall, H., Suhara, T., Karlsson, P., Nakashima, Y. & Swahn, C.G. (1995). Carbon-11-FLB 457: a radioligand for extrastriatal D2 dopamine receptors. *J Nucl Med*, **36,** 1275-81.

Halldin, C., Gulyas, B., Langer, O. & Farde, L. (2001). Brain radioligands–state of the art and new trends. *Q J Nucl Med*, **45,** 139-52.

Hamm, H.E. (1998). The many faces of G protein signaling. *J Biol Chem*, **273,** 669-72.

Happe, H.K., Bylund, D.B. & Murrin, L.C. (2001). Agonist-stimulated [^{35}S]GTPγS autoradiography: optimization for high sensitivity. *Eur J Pharmacol*, **422,** 1-13.

He, L., Di Monte, D.A., Langston, J.W. & Quik, M. (2000). Autoradiographic analysis of dopamine receptor-stimulated [^{35}S]GTPγS binding in rat striatum. *Brain Res*, **885,** 133-6.

Heimer, L. (2003). A new anatomical framework for neuropsychiatric disorders and drug abuse. *Am J Psychiatry*, **160,** 1726-39.

Henze, E., Huang, S.C., Ratib, O., Hoffman, E., Phelps, M.E. & Schelbert, H.R. (1983). Measurements of regional tissue and blood-pool radiotracer concentrations from serial tomographic images of the heart. *J Nucl Med*, **24,** 987-96.

Herrero, P., Markham, J. & Bergmann, S.R. (1989). Quantitation of myocardial blood flow with $H_2{}^{15}O$ and positron emission tomography: assessment and error analysis of a mathematical approach. *J Comput Assist Tomogr*, **13,** 862-73.

Hietala, J., Syvalahti, E., Vuorio, K., Rakkolainen, V., Bergman, J., Haaparanta, M., Solin, O., Kuoppamaki, M., Kirvela, O., Ruotsalainen, U. & et al. (1995). Presynaptic dopamine function in striatum of neuroleptic-naive schizophrenic patients. *Lancet*, **346,** 1130-1.

Hilf, G., Gierschik, P. & Jakobs, K.H. (1989). Muscarinic acetylcholine receptor-stimulated binding of guanosine 5'-O-(3-thiotriphosphate) to guanine-nucleotide-binding proteins in cardiac membranes. *Eur J Biochem*, **186,** 725-31.

Hoffman, E.J., Dahlblom, M., Ricci, A.R. & Weinberg, I.N. (1986). Examination of the role detection systems in quantitation and image quality in PET. *IEEE Trans Nucl Sci*, **NS-33,** 420-424.

Hoffman, E.J., Huang, S.C. & Phelps, M.E. (1979). Quantitation in positron emission computed tomography: 1. Effect of object size. *J Comput Assist Tomogr*, **3,** 299-308.

Hoffman, E.J., Huang, S.C., Plummer, D. & Phelps, M.E. (1982). Quantitation in positron emission computed tomography: 6. effect of nonuniform resolution. *J Comput Assist Tomogr*, **6,** 987-99.

Hurd, Y.L., Suzuki, M. & Sedvall, G.C. (2001). D1 and D2 dopamine receptor mRNA expression in whole hemisphere sections of the human brain. *J Chem Neuroanat*, **22,** 127-37.

Huynh, H. & Feldt, L. (1976). Estimation of the box correction for degrees of freedom from sample data in the randomized block and split plot designs. *Journal of Educational Statistics*, **1,** 69-82.

Jope, R.S., Song, L., Grimes, C.A., Pacheco, M.A., Dilley, G.E., Li, X., Meltzer, H.Y., Overholser, J.C. & Stockmeier, C.A. (1998). Selective increases in phosphoinositide signaling activity and G protein levels in postmortem brain from subjects with schizophrenia or alcohol dependence. *J Neurochem*, **70,** 763-71.

Joyce, J.N. (2001). Dopamine D_3 receptor as a therapeutic target for antipsychotic and antiparkinsonian drugs. *Pharmacol Ther*, **90,** 231-59.

Joyce, J.N., Ryoo, H.L., Beach, T.B., Caviness, J.N., Stacy, M., Gurevich, E.V., Reiser, M. & Adler, C.H. (2002). Loss of response to levodopa in Parkinson's disease and co-occurrence with dementia: role of D_3 and not D_2 receptors. *Brain Res*, **955,** 138-52.

Kaasinen, V. & Rinne, J.O. (2002). Functional imaging studies of dopamine system and cognition in normal aging and Parkinson's disease. *Neurosci Biobehav Rev*, **26,** 785-93.

Kapur, S. & Seeman, P. (2001). Ketamine has equal affinity for NMDA receptors and the high-affinity state of the dopamine D_2 receptor. *Biol Psychiatry*, **49,** 954-7.

Karlsson, P., Farde, L., Halldin, C., Swahn, C.G., Sedvall, G., Foged, C., Hansen, K.T. & Skrumsager, B. (1993). PET examination of [^{11}C]NNC 687 and [^{11}C]NNC 756 as new radioligands for the D_1-dopamine receptor. *Psychopharmacology (Berl)*, **113,** 149-56.

Kasai, K., Shenton, M.E., Salisbury, D.F., Onitsuka, T., Toner, S.K., Yurgelun-Todd, D., Kikinis, R., Jolesz, F.A. & McCarley, R.W. (2003). Differences and similarities in insular and temporal pole MRI gray matter volume abnormalities in first-episode schizophrenia and affective psychosis. *Arch Gen Psychiatry*, **60,** 1069-77.

Kebabian, J.W. & Calne, D.B. (1979). Multiple receptors for dopamine. *Nature*, **277,** 93-6.

Kessler, R.M., Ellis, J.R., Jr. & Eden, M. (1984). Analysis of emission tomographic scan data: limitations imposed by resolution and background. *J Comput Assist Tomogr*, **8,** 514-22.

Kessler, R.M., Whetsell, W.O., Ansari, M.S., Votaw, J.R., de Paulis, T., Clanton, J.A., Schmidt, D.E., Mason, N.S. & Manning, R.G. (1993). Identification of extrastriatal dopamine D_2 receptors in post mortem human brain with [^{125}I]epidepride. *Brain Res*, **609,** 237-43.

Khan, S.M., Smith, T.S. & Bennett, J.P., Jr. (1999). Effects of single and multiple treatments with L-dihydroxyphenylalanine (L-DOPA) on dopamine receptor-G protein interactions and supersensitive immediate early gene responses in striata of rats after reserpine treatment or with unilateral nigrostriatal lesions. *J Neurosci Res*, **55,** 71-9.

Kiss, B., Laszlovszky, I. & Auth, F. (2000). Neurochemical characterization of RGH-1756, a potent ligand of dopamine D_3 receptors. In *Int. J. Neuropsychopharmacology*, Vol. 3, Suppl. 1. pp. S135. XXIInd C.I.N.P. Congress: Bruxelles, Belgium.

Krishnan, K.R., Husain, M.M., McDonald, W.M., Doraiswamy, P.M., Figiel, G.S., Boyko, O.B., Ellinwood, E.H. & Nemeroff, C.B. (1990). In vivo stereological assessment of caudate volume in man: effect of normal aging. *Life Sci*, **47,** 1325-9.

Kuczenski, R. (1977). Differential effects of reserpine and tetrabenazine on rat striatal synaptosomal dopamine biosynthesis and synaptosomal dopamine pools. *J Pharmacol Exp Ther*, **201,** 357-67.

Kunzle, H. (1975). Bilateral projections from precentral motor cortex to the putamen and other parts of the basal ganglia. An autoradiographic study in Macaca fascicularis. *Brain Res*, **88,** 195-209.

Kunzle, H. (1977). Projections from the primary somatosensory cortex to basal ganglia and thalamus in the monkey. *Exp Brain Res*, **30,** 481-92.

Labbe, C., Froment, J.C., Kennedy, A., Ashburner, J. & Cinotti, L. (1996). Positron emission tomography metabolic data corrected for cortical atrophy using magnetic resonance imaging. *Alzheimer Dis Assoc Disord*, **10,** 141-70.

Lahti, R.A., Roberts, R.C. & Tamminga, C.A. (1995). D_2-family receptor distribution in human postmortem tissue: an autoradiographic study. *Neuroreport*, **6,** 2505-12.

Lammertsma, A.A., Bench, C.J., Hume, S.P., Osman, S., Gunn, K., Brooks, D.J. & Frackowiak, R.S. (1996). Comparison of methods for analysis of clinical [^{11}C]raclopride studies. *J Cereb Blood Flow Metab*, **16,** 42-52.

Lammertsma, A.A. & Hume, S.P. (1996). Simplified reference tissue model for PET receptor studies. *Neuroimage*, **4,** 153-8.

Langer, O., Gulyás, B., Sandell, J., Laszlovszky, I., Kiss, B., Domány, G., Ács, T., Farde, L. & Halldin, C. (2000). Radiochemical labelling of the dopamine D_3 receptor ligand RGH-1756. *J. Labelled Cpd. Radiopharm.*, **43,** 1069-1074.

Laruelle, M., Abi-Dargham, A., van Dyck, C.H., Gil, R., D'Souza, C.D., Erdos, J., McCance, E., Rosenblatt, W., Fingado, C., Zoghbi, S.S., Baldwin, R.M., Seibyl, J.P., Krystal, J.H., Charney, D.S. & Innis, R.B. (1996). Single photon emission computerized tomography imaging of amphetamine-induced dopamine release in drug-free schizophrenic subjects. *Proc Natl Acad Sci U S A*, **93,** 9235-40.

Laszlovszky, I., Kiss, B., Csejtei, M., Kovács, K.J., Auth, F., Sághy, K., Laszy, J. & Gyertyán, I. (2000). Neurochemical and behavioural properties of RGH-1756, a D_3 dopamine receptor ligand. In *Soc Neurosci Abst*. **26**. pp. 2328. Soc Neurosci.

Lazareno, S. (1999). Measurement of agonist-stimulated [^{35}S]GTPγS binding to cell membranes. *Methods Mol Biol*, **106,** 231-45.

Lefkowitz, R.J., Cotecchia, S., Samama, P. & Costa, T. (1993). Constitutive activity of receptors coupled to guanine nucleotide regulatory proteins. *Trends Pharmacol Sci*, **14,** 303-7.

Levant, B. (1995). Differential sensitivity of [^{3}H]7-OH-DPAT-labeled binding sites in rat brain to inactivation by N-ethoxycarbonyl-2-ethoxy-1,2-dihydroquinoline. *Brain Res*, **698,** 146-54.

Levant, B. (1998). Differential distribution of D_3 dopamine receptors in the brains of several mammalian species. *Brain Res*, **800,** 269-74.

Levesque, D., Diaz, J., Pilon, C., Martres, M.P., Giros, B., Souil, E., Schott, D., Morgat, J.L., Schwartz, J.C. & Sokoloff, P. (1992). Identification, characterization, and localization of the dopamine D_3 receptor in rat brain using 7-[^{3}H]hydroxy-N,N-di-n-propyl-2-aminotetralin. *Proc Natl Acad Sci U S A*, **89,** 8155-9.

Links, J.M. & Wagner, H.N., Jr. (1982). Specification of performance of positron emission tomography scanners. *J Nucl Med*, **23,** 82.

Logothetis, D.E., Kurachi, Y., Galper, J., Neer, E.J. & Clapham, D.E. (1987). The βγ subunits of GTP-binding proteins activate the muscarinic K^+ channel in heart. *Nature*, **325,** 321-6.

Maeda, J., Suhara, T., Ogawa, M., Okauchi, T., Kawabe, K., Zhang, M.R., Semba, J. & Suzuki, K. (2001). In vivo binding properties of [carbonyl-^{11}C]WAY-100635: effect of endogenous serotonin. *Synapse*, **40,** 122-9.

Maes, F., Collignon, A., Vandermeulen, D., Marchal, G. & Suetens, P. (1997). Multimodality image registration by maximization of mutual information. *IEEE Transactions On Medical Imaging,* **16,** 187-198.

Malmberg, A., Mikaels, A. & Mohell, N. (1998). Agonist and inverse agonist activity at the dopamine D_3 receptor measured by guanosine 5'-[γ-thio]triphosphate-[^{35}S] binding. *J Pharmacol Exp Ther*, **285,** 119-26.

Marquardt, D. (1963). An algorithm for least-squares estimation on non-linear parameters. *J Soc Ind Appl Math*, **11,** 431-441.

Martinez, D., Slifstein, M., Broft, A., Mawlawi, O., Hwang, D.R., Huang, Y., Cooper, T., Kegeles, L., Zarahn, E., Abi-Dargham, A., Haber, S.N. & Laruelle, M. (2003). Imaging human mesolimbic dopamine transmission with positron emission tomography. Part II: amphetamine-induced dopamine release in the functional subdivisions of the striatum. *J Cereb Blood Flow Metab*, **23,** 285-300.

Mawlawi, O., Martinez, D., Slifstein, M., Broft, A., Chatterjee, R., Hwang, D.R., Huang, Y., Simpson, N., Ngo, K., Van Heertum, R. & Laruelle, M. (2001). Imaging human mesolimbic dopamine transmission with positron emission tomography: I. Accuracy and precision of D_2 receptor parameter measurements in ventral striatum. *J Cereb Blood Flow Metab*, **21,** 1034-57.

Meltzer, C.C., Leal, J.P., Mayberg, H.S., Wagner, H.N., Jr. & Frost, J.J. (1990). Correction of PET data for partial volume effects in human cerebral cortex by MR imaging. *J Comput Assist Tomogr*, **14,** 561-70.

Mintun, M.A., Raichle, M.E., Kilbourn, M.R., Wooten, G.F. & Welch, M.J. (1984). A quantitative model for the in vivo assessment of drug binding sites with positron emission tomography. *Ann Neurol*, **15,** 217-27.

Missale, C., Nash, S.R., Robinson, S.W., Jaber, M. & Caron, M.G. (1998). Dopamine receptors: from structure to function. *Physiol Rev*, **78,** 189-225.

Muller-Gartner, H.W., Links, J.M., Prince, J.L., Bryan, R.N., McVeigh, E., Leal, J.P., Davatzikos, C. & Frost, J.J. (1992). Measurement of radiotracer concentration in brain gray matter using positron emission tomography: MRI-based correction for partial volume effects. *J Cereb Blood Flow Metab*, **12,** 571-83.

Murray, A.M., Ryoo, H.L., Gurevich, E. & Joyce, J.N. (1994). Localization of dopamine D_3 receptors to mesolimbic and D_2 receptors to mesostriatal regions of human forebrain. *Proc Natl Acad Sci U S A*, **91,** 11271-5.

Neer, E.J. (1995). Heterotrimeric G proteins: organizers of transmembrane signals. *Cell*, **80,** 249-57.

Newman-Tancredi, A., Cussac, D., Audinot, V., Pasteau, V., Gavaudan, S. & Millan, M.J. (1999). G protein activation by human dopamine D_3 receptors in high-expressing Chinese hamster ovary cells: A guanosine-5'-O-(3-[^{35}S]thio)- triphosphate binding and antibody study. *Mol Pharmacol*, **55,** 564-74.

Newman-Tancredi, A., Cussac, D., Brocco, M., Rivet, J.M., Chaput, C., Touzard, M., Pasteau, V. & Millan, M.J. (2001). Dopamine D_2 receptor-mediated G-protein activation in rat striatum: functional autoradiography and influence of unilateral 6-hydroxydopamine lesions of the substantia nigra. *Brain Res*, **920,** 41-54.

Niemann, K., Hammers, A., Coenen, V.A., Thron, A. & Klosterkotter, J. (2000). Evidence of a smaller left hippocampus and left temporal horn in both patients with first episode schizophrenia and normal control subjects. *Psychiatry Res*, **99,** 93-110.

Okada, F., Tokumitsu, Y., Takahashi, N., Crow, T.J. & Roberts, G.W. (1994). Reduced concentrations of the α-subunit of GTP-binding protein G_o in schizophrenic brain. *J Neural Transm Gen Sect*, **95,** 95-104.

Ollinger, J.M. & Fessler, J.A. (1997). Positron emission tomography. *IEEE Signal Processing Magazine*, **14,** 43-55.

Olsson, H., Halldin, C. & Farde, L. (2004). Differentiation of extrastriatal dopamine D2 receptor density and affinity in the human brain using PET. *Neuroimage*, **22,** 794-803.

Olsson, H., Halldin, C., Swahn, C.G. & Farde, L. (1999). Quantification of [^{11}C]FLB 457 binding to extrastriatal dopamine receptors in the human brain. *J Cereb Blood Flow Metab*, **19,** 1164-73.

Pakkenberg, B. (1990). Pronounced reduction of total neuron number in mediodorsal thalamic nucleus and nucleus accumbens in schizophrenics. *Arch Gen Psychiatry*, **47,** 1023-8.

Pakkenberg, B. (1992). The volume of the mediodorsal thalamic nucleus in treated and untreated schizophrenics. *Schizophr Res*, **7,** 95-100.

Paxinos, G.H., X-F. Toga, A-W. (2000). *The Rhesus Monkey Brain in Stereotaxic Coordinates*. Academic Press: San Diego, California.

Pennington, S.R. (1995). GTP-binding proteins 1: heterotrimeric G proteins. *Protein Profile*, **2,** 167-315.

Phelps, M.E., Hoffman, E.J., Huang, S.C. & Ter-Pogossian, M.M. (1975). Effect of positron range on spatial resolution. *J Nucl Med*, **16,** 649-52.

Piggott, M.A., Marshall, E.F., Thomas, N., Lloyd, S., Court, J.A., Jaros, E., Costa, D., Perry, R.H. & Perry, E.K. (1999). Dopaminergic activities in the human striatum: rostrocaudal gradients of uptake sites and of D_1 and D_2 but not of D_3 receptor binding or dopamine. *Neuroscience*, **90,** 433-45.

Poyot, T., Conde, F., Gregoire, M.C., Frouin, V., Coulon, C., Fuseau, C., Hinnen, F., Dolle, F., Hantraye, P. & Bottlaender, M. (2001). Anatomic and biochemical correlates of the dopamine transporter ligand ^{11}C-PE2I in normal and parkinsonian primates: comparison with 6-[^{18}F]fluoro-L-dopa. *J Cereb Blood Flow Metab*, **21,** 782-92.

Primus, R.J., Thurkauf, A., Xu, J., Yevich, E., McInerney, S., Shaw, K., Tallman, J.F. & Gallagher, D.W. (1997). II. Localization and characterization of dopamine D_4 binding sites in rat and human brain by use of the novel, D_4 receptor-selective ligand [^{3}H]NGD 94-1. *J Pharmacol Exp Ther*, **282,** 1020-7.

Pruessner, J.C., Li, L.M., Serles, W., Pruessner, M., Collins, D.L., Kabani, N., Lupien, S. & Evans, A.C. (2000). Volumetry of hippocampus and amygdala with high-resolution MRI and three-dimensional analysis software: minimizing the discrepancies between laboratories. *Cereb Cortex*, **10,** 433-42.

Pugsley, T.A., Davis, M.D., Akunne, H.C., MacKenzie, R.G., Shih, Y.H., Damsma, G., Wikstrom, H., Whetzel, S.Z., Georgic, L.M., Cooke, L.W. & et al. (1995). Neurochemical and functional characterization of the preferentially selective dopamine D_3 agonist PD 128907. *J Pharmacol Exp Ther*, **275,** 1355-66.

Quarantelli, M., Berkouk, K., Prinster, A., Landeau, B., Svarer, C., Balkay, L., Alfano, B., Brunetti, A., Baron, J.C. & Salvatore, M. (2004). Integrated software for the analysis of brain PET/SPECT studies with partial-volume-effect correction. *J Nucl Med*, **45,** 192-201.

Quarantelli, M., Larobina, M., Volpe, U., Amati, G., Tedeschi, E., Ciarmiello, A., Brunetti, A., Galderisi, S. & Alfano, B. (2002). Stereotaxy-based regional brain volumetry

applied to segmented MRI: validation and results in deficit and nondeficit schizophrenia. *Neuroimage*, **17,** 373-84.

Rask, T., Dyrby, T., Comerci, M., Quarantelli, M., Alfano, B., Berkouk, K., Baron, J.C., Colchester, A., Hojjat, A., Knudsen, G.M., Paulson, O.B. & Svarer, C. (2004). PVElab: Software for correction of functional images for partial volume errors. In *NeuroImage*, Vol. 22, Suppl. 1. pp. WE 286. The 10th Annual Meeting Of The Organization For Human Brain Mapping, Budapest, Hungary.

Raz, N., Rodrigue, K.M., Kennedy, K.M., Head, D., Gunning-Dixon, F. & Acker, J.D. (2003). Differential aging of the human striatum: longitudinal evidence. *AJNR Am J Neuroradiol*, **24,** 1849-56.

Ricci, A., Vega, J.A., Mammola, C.L. & Amenta, F. (1995). Localisation of dopamine D_3 receptor in the rat cerebellar cortex: a light microscope autoradiographic study. *Neurosci Lett*, **190,** 163-6.

Rieck, R.W., Ansari, M.S., Whetsell, W.O., Jr., Deutch, A.Y. & Kessler, R.M. (2004). Distribution of dopamine D_2-like receptors in the human thalamus: autoradiographic and PET studies. *Neuropsychopharmacology*, **29,** 362-72.

Robinson, S.W. & Caron, M.G. (1996). Interaction of dopamine receptors with G proteins. In *The dopamine receptors*, Neve, K.A. & Neve, R.L. (eds) pp. 137-165. Humana Press Inc.: Totowa, NJ.

Roland, P.E., Graufelds, C.J., Wåhlin, J., Ingeman, L., Andersson, M., Ledberg, A., Pedersen, J., Åkerman, S., Dabringhaus, A. & Zilles, K. (1994). Human brain atlas: for high-resolution functional and anatomical mapping. *Hum Brain Map*, **1,** 173-184.

Rorden, C. & Brett, M. (2000). Stereotaxic display of brain lesions. *Behav Neurol*, **12,** 191-200.

Rousset, O.G., Deep, P., Kuwabara, H., Evans, A.C., Gjedde, A.H. & Cumming, P. (2000). Effect of partial volume correction on estimates of the influx and cerebral metabolism of 6-[^{18}F]fluoro-L-dopa studied with PET in normal control and Parkinson's disease subjects. *Synapse*, **37,** 81-9.

Rousset, O.G., Ma, Y. & Evans, A.C. (1998a). Correction for partial volume effects in PET: principle and validation. *J Nucl Med*, **39,** 904-11.

Rousset, O.G., Yilong, M.A., Wong, D.F. & Evans, A.C. (1998b). Pixel- versus region-based partial volume correction in PET. In *Quantitative functional brain imaging with positron emission tomography*, Carson, R., Herscovitch, P. & Daube-Witherspoon, M. (eds) pp. 67-75. Academic Press.

Ryoo, H.L., Pierrotti, D. & Joyce, J.N. (1998). Dopamine D_3 receptor is decreased and D_2 receptor is elevated in the striatum of Parkinson's disease. *Mov Disord*, **13,** 788-97.

Schotte, A., Janssen, P.F., Bonaventure, P. & Leysen, J.E. (1996). Endogenous dopamine limits the binding of antipsychotic drugs to D_3 receptors in the rat brain: a quantitative autoradiographic study. *Histochem J*, **28,** 791-9.

Schotte, A., Janssen, P.F., Gommeren, W., Luyten, W.H. & Leysen, J.E. (1992). Autoradiographic evidence for the occlusion of rat brain dopamine D_3 receptors in vivo. *Eur J Pharmacol*, **218,** 373-5.

Schwartz, J.C., Diaz, J., Pilon, C. & Sokoloff, P. (2000). Possible implications of the dopamine D_3 receptor in schizophrenia and in antipsychotic drug actions. *Brain Res Brain Res Rev*, **31,** 277-87.

Seabrook, G.R., Kemp, J.A., Freedman, S.B., Patel, S., Sinclair, H.A. & McAllister, G. (1994). Functional expression of human D_3 dopamine receptors in differentiated neuroblastoma x glioma NG108-15 cells. *Br J Pharmacol*, **111,** 391-3.

Sedvall, G. & Farde, L. (1995). Chemical brain anatomy in schizophrenia. *Lancet*, **346,** 743-9.

Seeman, P., Chau-Wong, M., Tedesco, J. & Wong, K. (1975). Brain receptors for antipsychotic drugs and dopamine: direct binding assays. *Proc Natl Acad Sci U S A*, **72,** 4376-80.

Seeman, P., Ko, F., Willeit, M., McCormick, P. & Ginovart, N. (2005). Antiparkinson concentrations of pramipexole and PHNO occupy dopamine $D_{2(high)}$ and $D_{3(high)}$ receptors. *Synapse*, **58,** 122-8.

Selemon, L.D. & Goldman-Rakic, P.S. (1985). Longitudinal topography and interdigitation of corticostriatal projections in the rhesus monkey. *J Neurosci*, **5,** 776-94.

Shaul, P.W. & Anderson, R.G. (1998). Role of plasmalemmal caveolae in signal transduction. *Am J Physiol*, **275,** L843-51.

Shrout, P. & Fleiss, J. (1979). Intraclass correlations: uses in assessing rater reliability. *Psychological Bulletin*, **86,** 420-428.

Sim, L.J., Selley, D.E. & Childers, S.R. (1995). In vitro autoradiography of receptor-activated G proteins in rat brain by agonist-stimulated guanylyl 5'-[γ-[^{35}S]thio]-triphosphate binding. *Proc Natl Acad Sci U S A*, **92,** 7242-6.

Sokoloff, P., Andrieux, M., Besancon, R., Pilon, C., Martres, M.P., Giros, B. & Schwartz, J.C. (1992). Pharmacology of human dopamine D_3 receptor expressed in a mammalian cell line: comparison with D_2 receptor. *Eur J Pharmacol*, **225,** 331-7.

Sokoloff, P., Giros, B., Martres, M.P., Bouthenet, M.L. & Schwartz, J.C. (1990). Molecular cloning and characterization of a novel dopamine receptor (D_3) as a target for neuroleptics. *Nature*, **347,** 146-51.

Sovago, J., Dupuis, D.S., Gulyas, B. & Hall, H. (2001). An overview on functional receptor autoradiography using [^{35}S]GTPγS. *Brain Res Brain Res Rev*, **38,** 149-64.

Stanwood, G.D., Artymyshyn, R.P., Kung, M.P., Kung, H.F., Lucki, I. & McGonigle, P. (2000a). Quantitative autoradiographic mapping of rat brain dopamine D3 binding with [^{125}I]7-OH-PIPAT: evidence for the presence of D3 receptors on dopaminergic and nondopaminergic cell bodies and terminals. *J Pharmacol Exp Ther*, **295,** 1223-31.

Stanwood, G.D., Lucki, I. & McGonigle, P. (2000b). Differential regulation of dopamine D2 and D3 receptors by chronic drug treatments. *J Pharmacol Exp Ther*, **295,** 1232-40.

Stoof, J.C. & Kebabian, J.W. (1981). Opposing roles for D-1 and D-2 dopamine receptors in efflux of cyclic AMP from rat neostriatum. *Nature*, **294,** 366-8.

Strange, P.G. (1999). Agonism and inverse agonism at dopamine D_2-like receptors. *Clin Exp Pharmacol Physiol Suppl*, **26,** S3-9.

Sunahara, R.K., Guan, H.C., O'Dowd, B.F., Seeman, P., Laurier, L.G., Ng, G., George, S.R., Torchia, J., Van Tol, H.H. & Niznik, H.B. (1991). Cloning of the gene for a human dopamine D_5 receptor with higher affinity for dopamine than D_1. *Nature*, **350,** 614-9.

Talairach, J. & Tournoux, P. (1988). *Co-planar stereotaxic atlas of the human brain*. Thieme Medical: New York.

Talvik, M., Nordstrom, A.L., Olsson, H., Halldin, C. & Farde, L. (2003). Decreased thalamic D_2/D_3 receptor binding in drug-naive patients with schizophrenia: a PET study with [^{11}C]FLB 457. *Int J Neuropsychopharmacol*, **6,** 361-70.

Ter-Pogossian, M.M., Phelps, M.E., Hoffman, E.J. & Mullani, N.A. (1975). A positron-emission transaxial tomograph for nuclear imaging (PETT). *Radiology*, **114,** 89-98.

Vallone, D., Picetti, R. & Borrelli, E. (2000). Structure and function of dopamine receptors. *Neurosci Biobehav Rev*, **24,** 125-32.

Van Tol, H.H., Bunzow, J.R., Guan, H.C., Sunahara, R.K., Seeman, P., Niznik, H.B. & Civelli, O. (1991). Cloning of the gene for a human dopamine D_4 receptor with high affinity for the antipsychotic clozapine. *Nature*, **350,** 610-4.

Vanhauwe, J.F., Ercken, M., van de Wiel, D., Jurzak, M. & Leysen, J.E. (2000). Effects of recent and reference antipsychotic agents at human dopamine D_2 and D_3 receptor signaling in Chinese hamster ovary cells. *Psychopharmacology (Berl)*, **150,** 383-90.

Vanhauwe, J.F., Fraeyman, N., Francken, B.J., Luyten, W.H. & Leysen, J.E. (1999). Comparison of the ligand binding and signaling properties of human dopamine D_2 and D_3 receptors in Chinese hamster ovary cells. *J Pharmacol Exp Ther*, **290,** 908-16.

Videbaek, C., Toska, K., Scheideler, M.A., Paulson, O.B. & Moos Knudsen, G. (2000). SPECT tracer [^{123}I]IBZM has similar affinity to dopamine D2 and D3 receptors. *Synapse*, **38,** 338-42.

Watanabe, M., George, S.R. & Seeman, P. (1985). Regulation of anterior pituitary D_2 dopamine receptors by magnesium and sodium ions. *J Neurochem*, **45,** 1842-9.

Weiland, T. & Jakobs, K.H. (1994). Measurement of receptor-stimulated guanosine 5'-O-(γ-thio)triphosphate binding by G proteins. *Methods Enzymol*, **237,** 3-13.

Wienhard, K., Dahlbom, M., Eriksson, L., Michel, C., Bruckbauer, T., Pietrzyk, U. & Heiss, W.D. (1994). The ECAT EXACT HR: performance of a new high resolution positron scanner. *J Comput Assist Tomogr*, **18,** 110-8.

Willendrup, P., Pinborg, L.H., Hasselbach, S.G., Adams, K.H., Stahr, K., Knudsen, G.M. & Svarer, C. (2004). Assessment of the precision in co-registration of structural MR images and PET images with localized binding. In *International Congress Series*, Iida, H., Shah, N.J., Hayashi, T., Watabe, H. (ed), Vol. 1265. pp. 275-280. Elsevier B.V. Quantitation in Biomedical Imaging with PET and MRI. Proceedings of the International Workshop on Quantitation in Biomedical Imaging with PET and MRI, Osaka, Japan, 26 - 27 January 2004.

Wong, D.F. (2002). In vivo imaging of D_2 dopamine receptors in schizophrenia: the ups and downs of neuroimaging research. *Arch Gen Psychiatry*, **59,** 31-4.

Wong, D.F., Wagner, H.N., Jr., Tune, L.E., Dannals, R.F., Pearlson, G.D., Links, J.M., Tamminga, C.A., Broussolle, E.P., Ravert, H.T., Wilson, A.A. & et al. (1986). Positron emission tomography reveals elevated D_2 dopamine receptors in drug-naive schizophrenics. *Science*, **234,** 1558-63.

Yamaguchi, T., Kanno, I., Uemura, K., Shishido, F., Inugami, A., Ogawa, T., Murakami, M. & Suzuki, K. (1986). Reduction in regional cerebral metabolic rate of oxygen during human aging. *Stroke*, **17,** 1220-8.

Yang, C.Q., Kitamura, N., Nishino, N., Shirakawa, O. & Nakai, H. (1998). Isotype-specific G protein abnormalities in the left superior temporal cortex and limbic structures of patients with chronic schizophrenia. *Biol Psychiatry*, **43,** 12-9.

Yasuno, F., Suhara, T., Okubo, Y., Sudo, Y., Inoue, M., Ichimiya, T., Takano, A., Nakayama, K., Halldin, C. & Farde, L. (2004). Low dopamine D_2 receptor binding in subregions of the thalamus in schizophrenia. *Am J Psychiatry*, **161,** 1016-22.

Yokoi, F., Rousset, O.G., Dogan, A.S., Marenco, S., Evans, A.C., Gjedde, A.H. & Wong, D.F. (1998). Impact of partial volume effect correction on kinetic parameters: Preliminary experience in patient studies. In *Quantitative functional brain imaging with positron emission tomography*, Carson, R., Herscovitch, P. & Daube-Witherspoon, M. (eds). pp 77-82. Academic Press: San Diego.